School of Mathematics, Computer Science and Engineering
Department of Mechanical Engineering and Aeronautics

MEng Aeronautical Engineering: ETM071 MEng Design Project

FINAL DESIGN REPORT: BMFA Payload Challenge

17th June 2018

Supervisors

Professor Chris Atkin & Dr Chetan Jagadeesh

Project Manager

Maryam Mohamed

Project Engineer

Filip Livancic

Team

Thomas Agars, Sangiv Giovanni, Sherina Patel & Kalon De Silva

Contents

Nomenclature

AR – Aspect Ratio

b – Wing Span

C_{D0} – Zero Lift Drag Coefficient

C_L – Lift Coefficient

C_{LMAX} – Maximum Lift Coefficient

D – Drag

E_{BATT} – Battery Energy

C_{BATT} – Battery Coefficient

CE – Energy Density

C_{OWE} – Operating Weight Empty Coefficient

C_{MTOW} – Maximum Take-Off Weight Coefficient

C_P – Power Coefficient

C_T – Thrust Coefficient

η_0 – Propulsive Efficiency

h – Altitude

J – Advance Ratio

k – Lift Dependant Drag Coefficient

K – Lift Induced Drag Factor

L – Lift

l_h – Horizontal Tail CG Arm

l_v – vertical tail CG Arm

M1 – Mission 1

M2 – Mission 2

M3 – Mission 3

Re – Reynolds Number

n – Load Factor

P – Power

P/W – Power to Weight Ratio

q – Dynamic Pressure

S_{ref} – Wing Surface Area

v – Residual Rate of Climb

V – Velocity

V_h – Horizontal Tail Volume Coefficient

V_v – Vertical Tail Volume Coefficient

W/S – Wing Loading

W_{BATT} – Battery weight

W_{gear} – Landing Gear Weight

W_{pay} – Payload Weight

W_{motor} – Motor Weight

STOFL – Take-Off Field Length

ACRONYMS

AIAA – American Institute of Aeronautics and Astronautics

AOA – Angle of Attack

BMFA – British Model Flying Association

DBF – Design Build Fly

FAR – Federal Aviation Administration

HTP – Horizontal Tail Plane

Li-Po – Lithium Polymer

LRU – Line Replacement Unit

MAC – Mean Aerodynamic Chord

MEng – Master of Engineering

MTOW – Maximum Take-Off Weight

NiMH – Nickle Metal Hydroxide

NACA – National Advisory Committee for Aeronautics

OWE – Overall Weight Empty

PAX – Passengers

RAC – Rated Aircraft Cost

RC- Radio Controlled

RPM – Revolutions Per Minute.

TMS – Total Mission Score

TOFL – Take off Field Length

UAV – Unmanned Air Vehicle

VTP – Vertical Tail Plane

List of Figures

List of Tables

Tables and Figures in Appendix

List of Equations

1 Introduction

1.1 Aims and Objectives

The 2017/2018 MEng Aero design project was to design and build an aircraft to enter the 2018 BMFA Payload Challenge 5. The first term involved carrying out a conceptual design of a dual purpose regional and business aircraft for the AIAA DBF competition, an American counterpart. The analysis tools and techniques gained in the first term were then utilised for the BMFA competition. The objective of the BMFA Payload Challenge 5 was to carry the greatest mass of water in a single flight round where the score relied heavily on maximising the value of the ratio ''payload/aircraft empty mass''. Therefore, one of the most important considerations in both designs was weight reduction. The aim to build and fly an aircraft should illustrate the existing aeronautical and engineering knowledge gained in previous years, while also allowing the team to experience manufacture/ test/ operation phases. An additional aim was to meet the learning outcomes, mandated by the Engineering Council for MEng Programmes, relating to team work, management and leadership.

The academic objectives include utilising existing aeronautical knowledge to complete an in-depth conceptual analysis and implement knowledge from other fields such as propulsion, flight dynamics and structural analysis. Skills should be developed regarding with use of software packages such as AutoCAD, Excel, MATLAB, SolidWorks, and XFLR. All members of the team were required to meet milestones which were set by the project manager or supervisor. Appropriate and swift action was taken in the event of unforeseen circumstances with the view of resolving issues effectively to enable the project to move forward. A year-long collaboration involving continuous communication, organisational leadership, intellectual understanding, and reflective practices was a core objective of personal and professional growth for all team members.

The technical objective for 1st term was to employ previous design tools and resources to produce a conceptual design for AIAA mission specification. Conducting a parametric scoring analysis to determine optimum payload was required due to the complexity of mission rules. The MTOW, OWE, performance estimates, aerofoil selection and key dimensions were defined and reported before moving into the 2nd term.

The focus was then placed on the BMFA Payload Challenge 5, where the first objective was to adapt the conceptual design tools and resources to meet the new specification. A specific objective at this stage was to enhance preliminary design such as component sizing, aerodynamic analysis and propulsion selection as this area was significantly weak during the 1st term. A detailed design for all components had to be produced in order to manufacture within a set time period and budget.

As well as the academic and technical objectives all team members began the project with their own personal objectives.

“Providing effective leadership structure for the team through communication, delegation, building working relationships, managing conflicts and time while also developing individual knowledge of design.” – Maryam Mohamed

“Improve my capacity for being a team based and versatile Design Engineer.” – Thomas Agars

“Overall, my objectives for the project were to further improve my knowledge that I've learnt over the past 4 years and apply it to a real-life project, and I feel that taking part in this project has helped me achieve my goals.” – Kalon De Silva

“To learn about mechanical design and manufacturing techniques to create a functional aircraft.” – Filip Livancic

“Focus on personal development through working with members of the team to make high quality decisions together and reduce the number of negative confrontations with team members.” – Sherina Patel

“To successfully apply my team working and technical skills with the acquired knowledge from this course to design and build a competitive UAV as required by the specifications set by the competition of interest.” – Sangiv Giovanni

1.2 Design Process

The design process was broken up into conceptual and preliminary phases. The conceptual phase involved evaluating competition scoring rules. The scoring analysis for the BMFA was straightforward as only two variables were influential: payload and aircraft empty mass. The scoring analysis identified an optimum payload weight. When completing a conceptual aircraft design for the AIAA, various conceptual tools were generated such as weight correlations and an aircraft sizing chart. Weight correlations were obtained from data, collected from previous aircraft in the AIAA. Simultaneously, flight mechanic equations were used to establish a set of constraints for P/W and W/S. These values were displayed on an aircraft sizing chart from which a design point that satisfies all the constraints was selected. The AIAA scoring analysis shifted the design to a low weight model. This was untrue for the BMFA competition score and the weight correlations and aircraft sizing chart were adapted to correspond to the BMFA design criteria. Following the design point selection and optimum payload weight value, the first weight estimate of MTOW was completed. This concluded the conceptual design process.

The preliminary design phase involved an assessment of structural configurations, materials along with aerodynamic, stability and structural analysis of various components. A normalised

wing and tail-plane planform was constructed on excel. This identified the effects of AR and tapering, while providing wing and tail-plane geometry. Once geometries were determined and materials were decided, design of the aircraft began on SolidWorks. Calculations were completed to establish control surface sizing, this allowed the required torque for each control surface to be found and servos to be selected.

Various aerofoil geometries were also analysed using XFLR5 to select an aerofoil best suited for the competition. The characteristics judged were lift, drag and pitching moment. 3D analysis was implemented to further analyse the effect of AR and taper ratio. Concurrent to the aerodynamic analysis, a CG estimate was completed by scaling component geometries to weights from a similar MTOW AIAA aircraft. Powertrain analysis was also completed to identify an appropriate propeller blade diameter and pitch. Finally, various propellers were tested with the specified motor and battery as per the BMFA competition requirements.

Subsequently, the final design phase commenced. Detailed drawings of all components were completed on SolidWorks. At the same time, materials were finalised, and a procurement plan was devised. These were swiftly ordered and the first prototype (V1) was built within a week. A design review on the first prototype took place shortly and identified several areas for improvement. This lead to a design revaluation and prototype two (V2), which passed scrutineering and resulted in the final design.

1.3 Summary of predicted performance

The following table shows various performance values of the aircraft for all three rounds of the competition.

	Round 1	Round 2	Round 3
Score	30	69.36	161.85
MTOW (kg)	1.24	3.65	5.71
$W_{PAYLOAD}$ (kg)	0	1.5	3.5
Required Power (W)	72.75	215.12	336.13
Cruise Speed (m/s)	9.05	15.55	20.44
Take-off Speed (m/s)	5.65	9.72	15.23
Stall Speed (m/s)	4.71	8.10	10.13
Turn Radius (m)	8.34	24.66	38.54
Wing Loading (Pa)	18.34	54.27	84.80

Table 1.1: Predicted performance for the aircraft in all three rounds.

The total flight score predicted in the competition is 261.21 with a 1.73kg aircraft empty mass. Refer to section Scoring System Analysis for calculations and the Appendix for rules. A 1.5kg payload is attempted in round 2 held by a bottle placed within the fuselage. An additional 2kg payload is attempted in round 3 carried with wing tanks. The maximum required power is 336.13W. V_{STALL} is determined from MTOW and $C_{L\,MAX,\,CLEAN}$ (1.35). V_{TO} is 20% faster than V_{STALL}, whilst V_{CRUISE} is estimated at approximately 60% faster than V_{TO}. The turn radius is calculated at V_{CRUISE}. W/S changes significantly from 18.34Pa to 84.80Pa in round 1 to round 3

respectively. The greatest value of W/S in round 3 does not however exceed the stall W/S which occurs at 114.66Pa. W/S is discussed in further detail in section Aircraft Sizing Process. The batter, motor and controller were specified in the rules whilst the propeller size was selected based on testing as shown in section Powertrain Analysis.

Battery	Motor	Controller	Propeller	Blade Count
3S LiPo	E-flight Power 10	E-flight 40A	12”x6”	2

Table 1.2: Powertrain components.

Uncertainties in performance arise from the battery as the variation of voltage and current throughout the flight is unknown. The wind speed is predicted through analysing the average wind speed in Lincolnshire. This is shown as Fig.A1 in the Appendix. Applying a 90% confidence interval, the wind speed in June 2018 is predicted between 6.14-8.57kts.
The key wing properties and dimensions are outlined in the table below.

Aerofoil	AR	Taper Ratio	Span	Root Chord	Tip Chord	MAC	Dihedral
Clark - Y 11%	6	0.6	1.991m	0.415m	0.249m	0.339m	3°

Table 1.3: Wing geometry.

The values can be assumed to be accurate as many of the initial assumptions during conceptual design were confirmed or updated during the preliminary design stage. The initial wing design was weak and easily twisted. The wing was redesigned, increasing the number of interlocking components, strengthening the entire wing. A spar test was also conducted, refer to section Testing: Wing Spar. With the redesign, testing and ensuring the wing is built without twist, safe flight should be sustained.

	Volume Coefficient	AR	Taper Ratio	Span	Root Chord	Tip Chord	MAC
VTP	0.076	2	0.8	0.485m	0.269m	0.216m	0.243m
HTP	0.58	4	1	0.782m	0.195m	0.195m	0.195m

Table 1.4: Tail-plane geometry.

The tail-plane sizing process was based on approximated values, refer to section Preliminary Design: Tail-Plane. One aspect that was overlooked was the stiffness of the boom (length 0.85m) which is slightly unsteady.

2 Management

2.1 Organisation, Roles and Responsibilities

The Aero design team 2018 consists of 6 MEng Aeronautical Engineering students. The team was supervised by Professor Chris Atkin and Dr Chetan Jagadeesh. A matrix organisation structure of leadership was utilised, similar to the management hierarchy observed in most aeronautical companies. This integrated organisational structure allowed communication

between all members and supervisors. A change control systematic approach was implemented, with all major decisions run by the team supervisor. This resulted in prompt decision making and thus action when faced with unforeseen circumstances. Team meetings were held weekly to aid development, whilst meeting minutes and weekly individual reports were recorded to ensure all members were performing. The organisational structure for the 2018 competition is shown below.

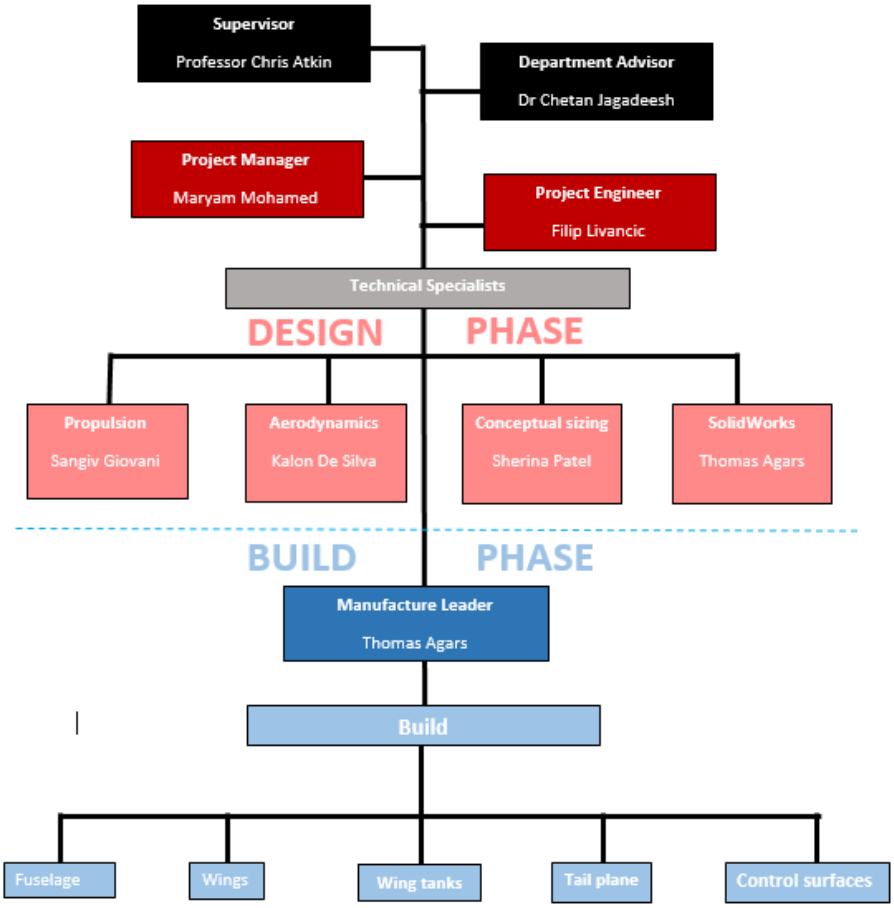

Figure 2.1 Hierarchy organisational chart.

The design phase was separated into individual tasks with the project manager and engineer assisting in all activities. The testing phase was conducted by all team members. The project manager's role was to manage team logistics through organisation of time and resources (people and budget), while also assessing quality and risks that may occur within the project. The project manager worked closely with the project engineer, whose role was to allocate and supervise all tasks in relation to design, build and test efforts. Guidance and suggestions when reaching milestones was provided to all team members by the supervisor and department advisor.

2.2 Project Breakdown Structure

A Gantt chart was established at the beginning of the design project to illustrate the tasks required to be accomplished, their estimated duration and highlight any major deadlines. The Gantt chart contained tasks relating to the design, manufacturing and test phase. This was maintained by the project manager throughout the project. Throughout the design and manufacturing phase, unplanned tasks emerged, and certain activity durations was either shorter or longer than planned. Therefore, the Gantt chart was continuously altered accordingly to reflect this. The Gantt chart is labelled Fig.A2 in the appendix, demonstrating all the activities and their subsequent durations during the design and build of the aircraft.

2.3 Expenditure

The budget for the year was £1000 and full record of purchased items is shown in the Appendix: Table A4. All items were grouped into categories and the cost of each category is shown below.

Category	Cost
Wood: Balsa, Ply and Dowels	£465.39
Wrap inc. Heat Adhesive	£125.34
Wing Tank Equipment	£239.39
Carbon Fibre inc. Landing Gear	£203.66
Hinge/Servo/Control Horns	£103.01
Propulsion/Electrical	£95.77
Glue	£62.23
Entry Fee	£50.00
Shipping	£152.28
TOTAL	**£1,497.07**

Table 2.1 Cost of items spent for the project.

The total cost this year was £1497.07 signifying the team overspent by 50% and therefore failing to meet cost objectives. The weightings of each category contributing to total cost is shown in the following chart.

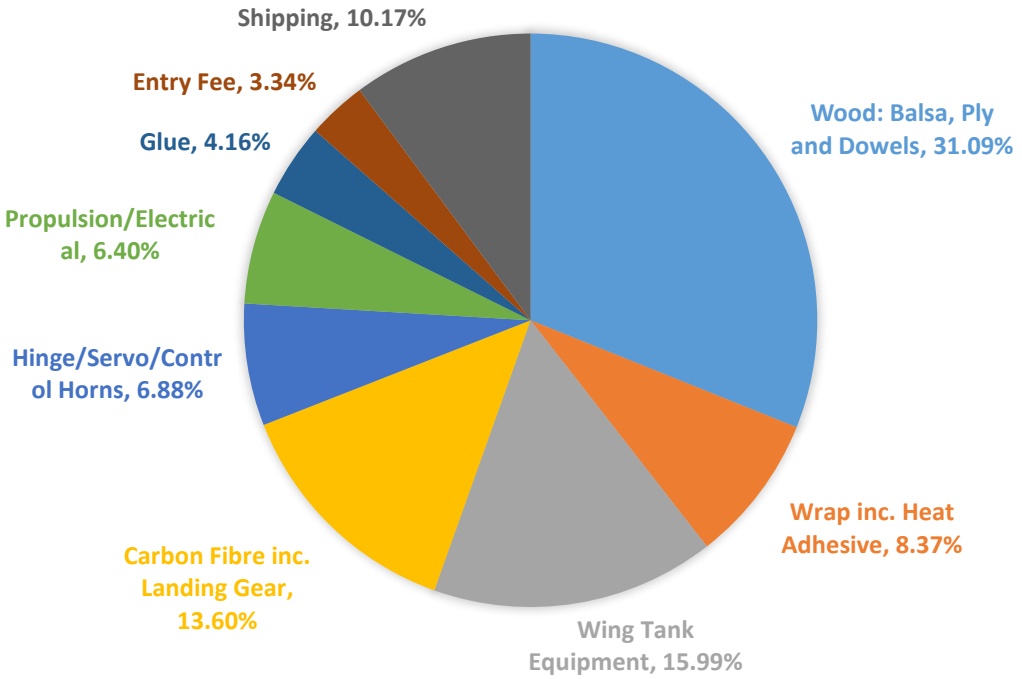

Figure 2.2 Pie chart showing area and weight of expenditure.

Expenditure was greatest for buying wood at 31.09% of total cost. This was a necessity and as the team were careful not to waste too much material, the cost for wood could have easily been much higher. The wing tank equipment was the second largest area of expenditure at 15.99% (£239.39). This could have been reduced if additional methods of carrying water payload were investigated. Shipping fees were unexpectedly higher than anticipated at £152.28. This amounted to 10.17% of total cost and the fourth greatest cost contributor. This may have been prevented if wood from Balsa Mart was bulk bought as the company had a standard shipping fee of £7.95. The team did manage to achieve minor savings such as £10 off when buying from Glue Guns Direct and £1.43 due to reward points at Hobby King.

3 Conceptual Design

3.1 Scoring System Analysis

The scoring rules outlined by the BMFA was the foundation for our design concept. There were three rounds in which the first was a qualification flight which carried no payload. The second and third round incorporate maximum payload attempt limits of 2.25kg and 4.5kg respectively. Refer to Appendix – Rules for further information. The scoring is defined below:

- **Score**: the score for a round (30 for a successful qualification flight in round 1).
- **Flight Score**: the sum of the score achieved in all three rounds.
- **Normalised Score**: A percentage of the best score achieved in the competition where the best score is equal to 100.

The score for round 2 and 3 is calculated using the following equation:

$$\frac{Payload}{Aircraft\ Empty\ Mass} \times 80$$

Equation 1 Scoring ratio

The aircraft empty mass is defined as the mass without payload, payload receptacle but with flight batteries. Based on the scoring equation, the design priority was to maximise the payload to aircraft empty mass ratio. The payload weight was determined in the initial stages of design, and the team actively aimed to minimise the aircraft empty mass throughout the design process.

To select a payload weight, the score was analysed to investigate how it is affected by payload. This is observed in the figure below.

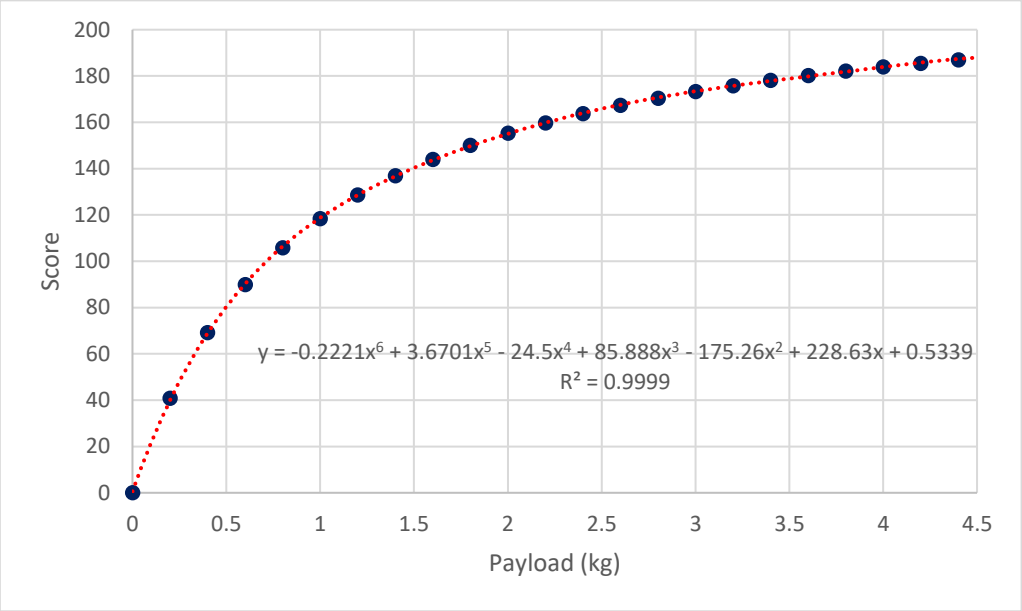

Figure 3.1 Flight score sensitivity to payload.

The graph was obtained by initially setting a range of payload values from 0kg to 4.5kg (maximum permissible payload) in increments of 200g. The MTOW could then calculated followed by the OWE. The aircraft empty mass was found by adding on the weight of the battery to the OWE for each value of payload. The weight calculations are outlined in section Weight Estimation. Once the aircraft empty mass was found, the corresponding score could be obtained from Eqn.1. Table A 1 in the Appendix shows the full results.

The relationship between the score and payload can be approximated by a 6th order polynomial trend with the equation shown in Fig.3.1. The correlation is extremely sensitive to the weight coefficients, C_{OWE} and C_{MTOW}, refer to section weight correlation which shows how they are obtained.

Increasing the payload by a consistent 200g does not reflect in a constant increase in flight score. Instead Fig.3.1 shows the incremental change in flight score reduces with larger values of payload. The benefits in carrying more payload become insignificant as the impact on score becomes negligible. Considering the maximum payload attempt limits, the team initially decided to opt for an aircraft able to carry 2kg in both rounds. This decision was based on the fact the flight score gain falls below 3% for any additional payload after 2kg. Refer to section Final Strategy which summarises how and why the initial payload strategy was adjusted.

The scoring analysis for the BMFA was very simple compared to the AIAA. The AIAA included complex scoring concepts which required the use of MATLAB to solve a 7 degree of freedom problem. The complexity allowed for a profound understanding on flight variable dependencies. The simplicity of the BMFA scoring was disappointing as the team had the skills required to solve a code which was much more complex. One significant difference between competitions was the wing span which for the AIAA, minimising the span was crucial to scoring however in the BMFA there was no limit.

3.2 Weight Correlation

The aircraft weight process requires the estimation of two key coefficients, C_{OWE} and C_{MTOW}. To obtain these parameters, aircraft weight data was correlated from the AIAA DBF and plotted on the following figure.

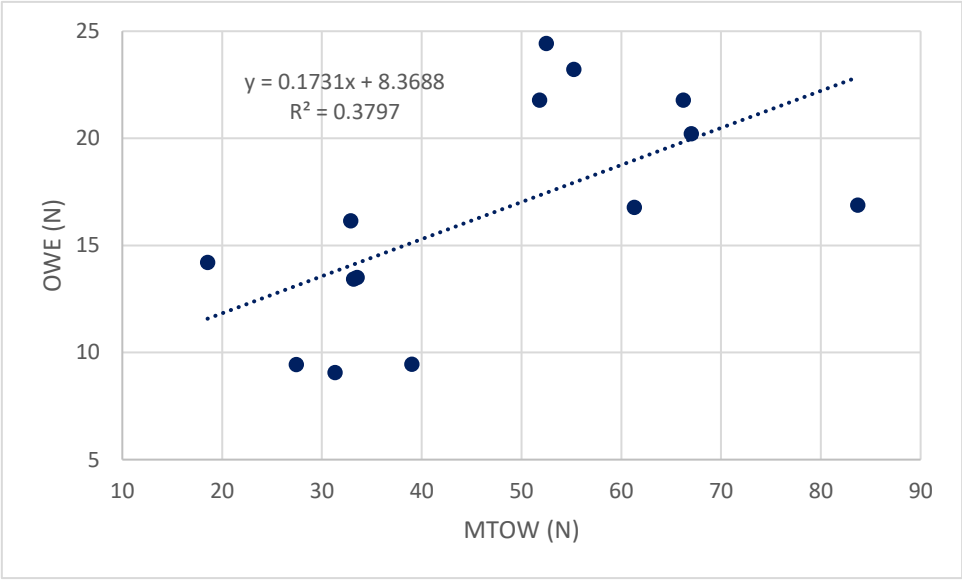

Figure 3.2 OWE and MTOW values for aircraft in the AIAA DBF database.

The OWE values in Fig.3.2 excludes the battery weight as the AIAA DBF allows a team to choose their own battery. Aquarius defines the OWE as the aircraft weight excluding batteries, payload and payload receptacles. Market research on AIAA competitor aircraft were compiled at the start of the project and suitable aircraft were selected based on the outcome of the scoring analysis. For the AIAA, only light weight models were required and so

aircraft with an OWE greater than 1kg were removed from the sample. However, for the BMFA, light weight models were excluded from the sample as well as aircraft which presented an OWE over 3kg. The data for the aircraft displayed in Fig.3.2 is shown in Table A 2 located in the Appendix A. The gradient of the trend line represents C_{MTOW} at 0.1731 and the intercept C_{OWE} is set at 8.3688N.

The relationship shown in Fig.3.2 shows a weak linear correlation between MTOW and OWE. The scatter is most likely present as the data was taken over several years and the aircraft were designed to perform different missions. As the flight score is greatly dependent on these parameters and, they are heavily used throughout conceptual design, it would have been desirable if the data presented a strong correlation. This would improve the accuracy of analysis. One method which was not investigated was to sort the data in terms of mission specification rather than a filter based on OWE.

3.3 Aircraft Sizing Process

An aircraft sizing chart is the first step in establishing the size of the aircraft. The chart identifies mission constraints in terms of P/W and W/S. A suitable design space is classified in which a design point for the challenge can be selected.

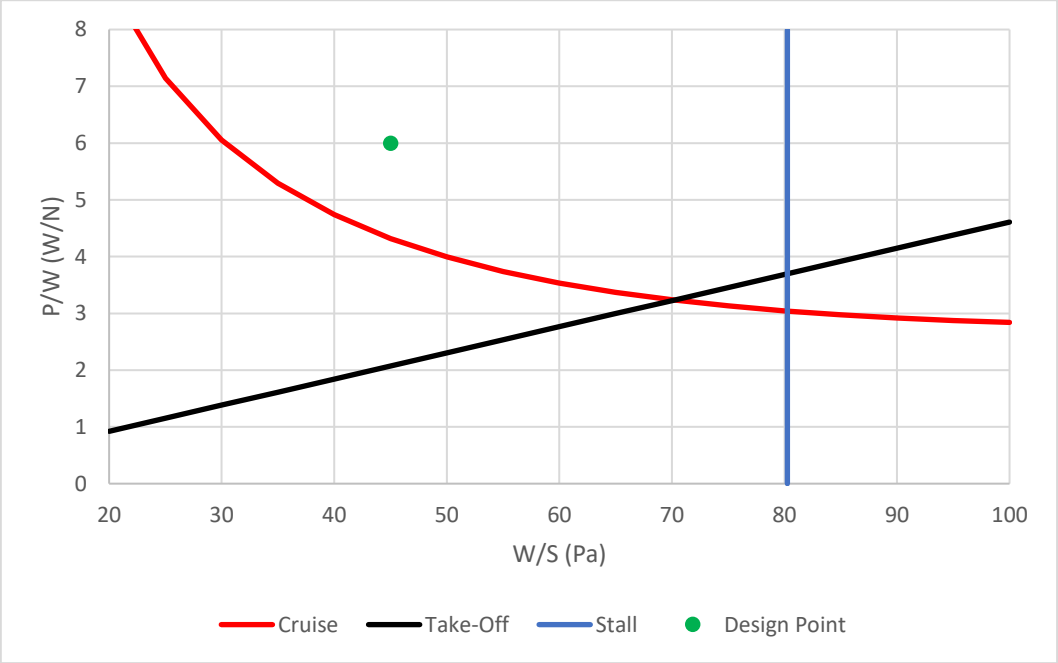

Figure 3.3 Aircraft Sizing Chart.

The three prime flight conditions considered for the aircraft sizing chart above were, take-off, cruise and stall; the speed parameters initially estimated for these conditions were 20m/s, 15m/s and 12m/s respectively. The aircraft must satisfy these constraints and they are calculated by manipulating the drag equation into different forms of P/W. All equations are shown in the Appendix.

All parameters were first predicted using aircraft from the AIAA DBF database. $C_{L\ MAX,\ CLEAN}$ was originally estimated at 1.3 and updated to 1.35 once the aerofoil analysis was completed in XFLR5. The aircraft is assumed to operate at standard sea level conditions at a density of approximately 1.225kg/m^3. The final parameters used are shown in the following table.

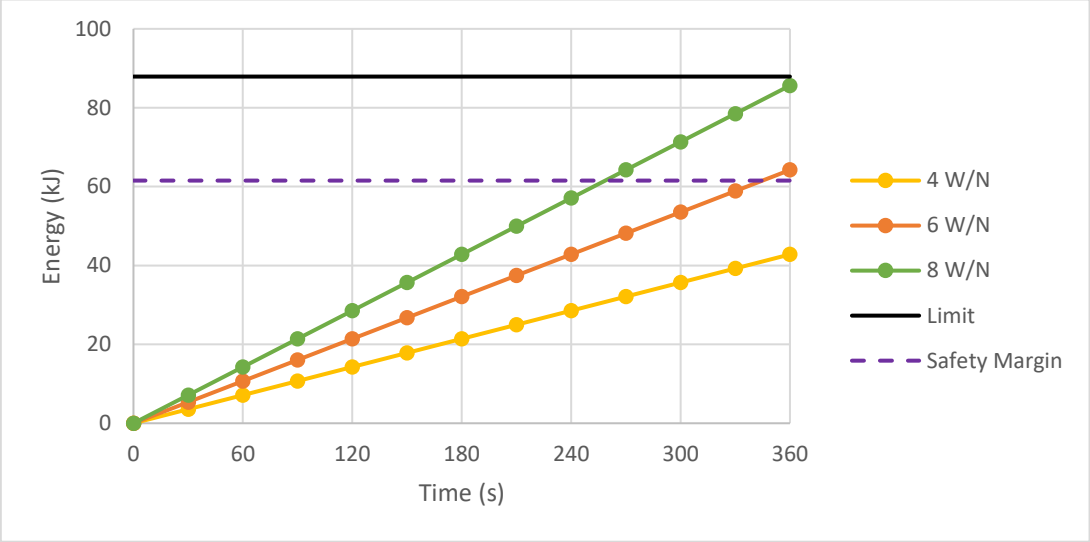

Figure 3.4: Effects of different P/W's on energy.

A 30% safety margin was implemented on the battery energy limit (87.9kJ) bringing the threshold down to 61.5kJ. A P/W of 4W/N is the most attractive as it remains well below the limits however from the aircraft sizing chart, this is only possible when W/S is above 50Pa.

Through analysing the battery, it was discovered that a 2kg payload value target was too conservative and the battery was able to endure a greater payload. The idea was explored of attending the competition with the ability to carry more payload even if the structure and size was designed for a 2kg payload. The relationship between W/S and payload was then investigated. It was found that if W/S is reduced as much as possible (close to the cruise constraint curve) then extra payload could be carried without the aircraft stalling. At a 45Pa W/S, the aircraft designed for 2kg was capable of an additional 1.5kg payload while only breeching the stall safety margin by 5.6%. A P/W of 4W/N was then no longer in the design space. A P/W of 6W/N then appeared the most viable as the battery can accommodate 6mins of flying time while only slightly surpassing the safety margin. If 5 W/N P/W were to be considered the design point would be located too close to the cruise constraint.

P/W (W/N)	W/S (Pa)
6	45

Table 3.1 Design point selection.

The design point is located away from all constraints which should ensure the aircraft complies within the boundaries of the flight envelope. The design point is used in conjunction with the weight estimation to determine the power and S_{REF}. S_{REF} is used to construct a wing planform which resolves key dimensions. The output values from the wing planform are then

used to solve the tail plane geometry.

The aircraft sizing chart ultimately decides every aspect of design and dimensions and therefore change must be carefully considered, controlled and communicated throughout the team. During the first term several aircraft sizing charts were developed and used simultaneously with no team member knowing which one was correct. This issue was omitted when the project manager put a password on the document and so all changes had to be communicated. This worked effectively during the second term and the technique should have been initiated from the start.

The sizing process worked well for both AIAA and BMFA specifications, but it is heavily dependent on assuming the input data is accurate. The accuracy improves over time as iterations are made, for example $C_{LMAX,\ FLAPPED}$ was originally set at 1.7. This was later reduced to 1.5 following aerodynamic analysis during preliminary design. The approach to selecting the design point was very different between the AIAA and BMFA however, there was one crucial similarity which was implementing safety margins to keep the design point away from the periphery of the design space. This ensured every time the sizing chart was updated, and the constraints relocated, the design point did not fall outside of the design space.

3.4 Final Strategy

As the aircraft was designed to carry a maximum payload of 3.5kg, this became the target for round 3 due to the 2.25kg limit in round 2. The initial 2kg target payload weight was reduced to 1.5kg. This was because a plastic bottle was decided for the payload receptacle and, a 1.5ltr bottle is more streamlined allowing for an aerodynamic fuselage profile. The final payload strategy was to carry 1.5kg in round 2 and 3.5kg in round 3. This decision is based on the analysis of the scoring system (section Scoring System Analysis), aerodynamic considerations and, the evaluation between W/S and payload (section Aircraft Sizing Process). Wing tanks were employed as the payload receptacle for the additional 2kg payload in round 3. The design of the tank is further outlined in section Wing Tanks. The implementation of wing tanks led to the re-evaluation of AR. The upper range on AR became limited as it affects the length of the root chord where the wing tank is slotted in. The geometry was critical as the tank should be minimised in the span-wise direction to avoid compromising the structure of the wing. It was determined that an AR of 6 was the maximum acceptable limit as any higher, the tank would not fit. As the AR was already set at 6, this did not need to be adjusted.

3.5 Weight Estimation

The aircraft weight sources arise from payload, batteries, airframe and powertrain. A circular dependency exists between these weight components.

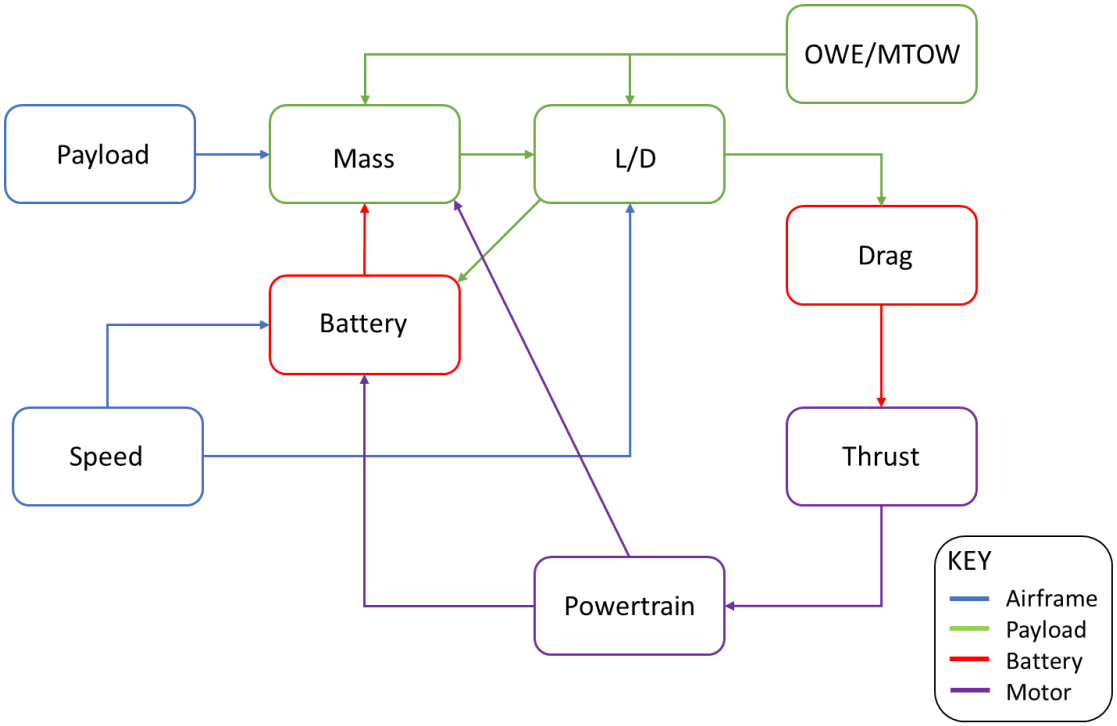

Figure 3.5 Aircraft weight source dependency.

The OWE includes weights such as landing gear, motor, electrics and glue as the AIAA aircraft account for these components. This leaves the battery weight and payload as the remaining principal components. For the purposes of weight estimation, it is assumed that

$$MTOW \approx OWE + W_{PAYLOAD} + W_{BATTERY}$$

Equation 2 Maximum weight composition

The OWE is expressed as

$$OWE = C_{OWE} + C_{MTOW} MTOW$$

Equation 3 OWE calculation

This is the trend shown in section weight correlation

Substituting the OWE expression into Eqn.2, the final MTOW equation for weight estimation is calculated as

$$MTOW = \frac{C_{OWE} + W_{payload} + W_{battery}}{1 - C_{MTOW}}$$

Equation 4 MTOW calculation

The MTOW is calculated for each round and the OWE is calculated using the greatest MTOW which is in round 3.

Component	Mass (kg)
$W_{PAYLOAD}$ R1	0
$W_{PAYLOAD}$ R2	1.5
$W_{PAYLOAD}$ R3	3.5
$W_{BATTERY}$	0.17
MTOW R1	1.24
MTOW R2	3.65
MTOW R3	5.71
OWE	1.56
Aircraft Empty Mass	1.73

Table 3.2 Aircraft mass data.

The OWE is predicted at 1.56kg and the aircraft empty mass is determined by adding on the weight of the battery. Every effort was made to find a 3S LiPo battery (2200 mah maximum capacity) with the lightest weight. The Overlander Supersport was purchased at a weight of 0.17kg. The aircraft empty mass is 1.73kg. A CAD based weight model was also simulated and the software estimated an OWE of 1.7kg which is only a 1.73% difference validating the accuracy of the calculations.

The first weight estimate for the BMFA was simple compared to the AIAA. Estimating the weight was the most challenging concept during the conceptual design phase for the AIAA. This was because the scoring algorithm developed, suggested the highest scoring configuration was a light weight model. The weight estimation does not work well for light weight aircraft and to solve this problem the OWE/MTOW trend line had to be refined. This involved extracting more weight components in addition to the payload and battery such as the motor, landing gear and servos. This essentially results in an airframe weight rather than an OWE. Had this of been completed, it would have likely resulted in a more reliable first weight estimate.

4 Preliminary Design

4.1 Configuration Selection and Materials

Configurations

The analysis of different UAV configurations and their suitability to a specific mission serves as the foundation to the design process. Furthermore, identifying ideal materials and manufacturing techniques necessary to build the UAV also must be closely considered before diving into the detailed design. For this project three general configurations were selected: Conventional, Flying wing, and Pod & Rod. For the purposes of illustration only, these configuration variants are shown below.

Variant 1: Conventional	Variant 2: Flying Wing	Variant 3: Pod + Rod
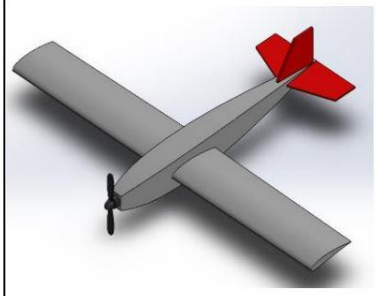	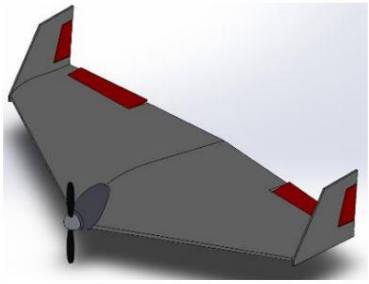	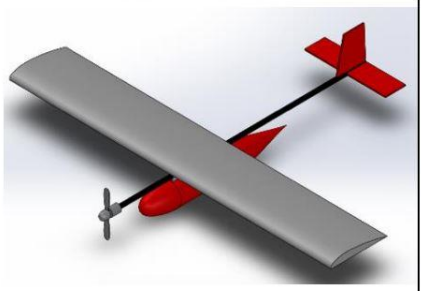

Figure 4.1 Configuration Variants.

In the preliminary design process, any of the above configurations could have been selected, however each configuration presented a different set of benefits and challenges.
The conventional approach entails the use of a space frame structure forming the full length of the fuselage and a centrally mounted wing with a standard horizontal/vertical tail plane. This approach would enable easily applied dynamic stability analysis in addition to simple CG balancing. The fuselage structure could be designed in such a way to carry large payloads, however the consequence of changing the detailed design of the fuselage during the prototype phase is that all other components would also require modification to fit the new fuselage.

A flying wing would remove the need for a tail plane assembly, however the absence of the tail plane would require a complex aerodynamic analysis to develop a stable design. The benefit of a flying wing is the potential to load the payload in a span wise direction, helping to reduce the significant bending moments at the wing roots.

The pod & rod design process is centred on the use of a carbon fibre rod replacing the traditional fuselage structure. This approach allows for more independent design of components with minimal effect on one another if specifications change. The pod, whereby the liquid payload is stored, must secure the weight of the payload while taking on aerodynamic loads. This requirement would be relatively easy to implement as any size 'pod' could be designed and attached to the underside of the rod, allowing for design change during prototyping phases.

Overall, the Pod and Rod configuration was selected to form the foundation of our design process. The reasons for this choice include: conventional aerodynamic analysis, simplified structural analysis and independent design of components - best suited to our mission requirements both in terms of learning outcomes, team dynamics and the BMFA mission.

Materials

Preliminary investigation revealed that typical materials used to build UAV's include: Balsa wood, plywood, 3D printing and composites such as carbon fibre and fibre glass.

Balsa wood is a low density, high strength material with highly attractive properties for model aircraft. This material exists in several grades, being ideal for use in wing ribs and spars, while also being suitable for leading edge skins whereby flexibility is necessary. With access to laser cutting facilities on campus, this material can be easily cut on site and constructed into light weight structures. Similarly, plywood can also be rapidly cut and constructed, however the material is 4-5x heavier than balsa. Plywood is significantly less anisotropic than balsa and should be used in critical load bearing locations.

Where components are relatively small yet highly complex, 3D printing can be of huge benefit. However, 3D printed thermoplastics are relatively heavy and can be highly vulnerable to shear forces along the printing layers when under load. Regarding this project, motor mounts, landing gear or even servo mounts are potential uses of 3D printing.
Carbon fibre has an impressive strength to weight ratio. Pre-formed carbon fibre tubes and sheets enable easy manufacture of structures. They could potentially be used as main structural elements such as booms or spars, or as reinforcement. For example, gluing carbon fibre to the external surface of the spar or ribs.

Fuselage
The fuselage includes the pod and any central structure used to connect the pod, boom and wing. The primary design consideration for this UAV was the minimisation of structural weight. As in any structural design, the structure was optimised throughout the prototyping phase. The baseline weight was largely determined by the overall design strategy and materials selected.

The initial design strategy discussions involved the design of major load bearing elements first, then adding reinforcements to strengthen any bending or torsional weaknesses. It was undecided whether the electronics should be mounted within the fuselage structure or simply onto the rod. In any case, glue joints alone were identified as insufficient, hence it was decided to interlock or jigsaw all components, removing the dependency on glue for joint strength.

Wings
Preliminary investigation revealed several potential wing design strategies. The most common involving a carbon main spar element extending through the full span of the wing and fuselage. Another involved I-beam structures built up of plywood, balsa and composite materials. Once again, the main design parameter was to be light weight. The difficulty was establishing which material choice could be made lighter while still being adequately strong yet not over engineered. After additional weight estimations it was discovered that plywood/balsa spar could be made lighter than a simple carbon spar, hence the decision to utilise plywood and balsa was made.

Wing Tanks

The greater the mass of water carried round the prescribed track the greater the score awarded to the aircraft for the BMFA flight challenge 5. The bottle mounted under the fuselage was ideal in shape in terms of aerodynamics as it is relatively slender whilst being able to hold 1.8kg of water. However, to score more points an attempt of heavier load was decided whilst maintaining the CG and balance of the aircraft.

The next step was deciding whether a pre-made catheter bag or a custom-made tank was best. The pre-made catheter bag was simple and easy as it needed no manufacturing effort whereas a custom-made water tank is difficult and time consuming to design and manufacture in terms of making the tank water-tight. The custom-made tank was finally decided as the appropriate solution due to the catheter bag having less control over how much volume could be carried in each bag. A design of unique wing tanks was also considerably more interesting and something unfamiliar to the team.

One of the most important limitations to consider was the empty weight restriction of the tanks which needed to be no more than 10% of their filled mass. To ensure the tanks met the weight restriction, the material had to be of low weight. To create a tank that would fit perfectly in the wing, the material had to be susceptible to being shaped, while remaining strong. The idea of polypropylene plastic came to light and after research was decided to be suitable for the final design.

Tail Plane

- Purpose

The essence of the tail plane is to balance the moments produced by the wing and the CoG. Due to the symmetry of the tail aerofoil geometry, the tail surface experiences a relatively neutral flow over the wing at a zero angle of attack. Stress is only exerted on the tail when the airflow is at a non zero angle of incidence due to resultant lift force over the surface. Though the stress at the tail is a small fraction of that experienced by the wing and therefore the strength of the tail plane is not as critical as the main wing. The appropriate tail volume coefficients and boom length will assist in trimming the aircraft. Any out of balance forces are undesireable due to elevator compansation which produces more drag, though can be avoided by having a relatively balanced aircraft. There were three main criteria in the design idea of the tailplane: lightweight, detachable and taxiable.

- Overall Tailplane Layout

An abundance of options are available in tail design, but for the purposes of simplicity it was decided the tail design was to follow a conventional style. To make the design as light as possible, the idea was to use plywood and carbon fibre sparingly due to their high material densities. The majority of the design was constructed from balsa wood. Plywood and carbon

were to be implemented into components which are thought to experience significant stress (e.g. spar, servo mount, tail landing hard point, boom attachment).

- Method of Attachment

The main challenge in design of the pod and rod was between the interface of the tail and the boom. To achieve safe and successful flight, the tail and the servo mechanisms would need to be securely attached to the carbon. One of the methods of attachment was to embed the tail surface into a plastic corner guard and bind the guard to the rod with some steel wire. However, an obvious disadvantage would be that that the tail surfaces would then be offset by the size of the carbon tube. The alternative was to make a "sleeve" that went around the carbon to secure it. This would keep the tail surfaces centralised. The sleeve concept was pushed forward and eventually developed into a plywood box with a pair of bolts securing the tail.

- Control Hinging and Actuation

There are many hinging methods for the actuation of the tail surfaces. Conventional hinging methods are certainly robust however, there are some alternative methods that are simpler and lighter. For instance, flexi-hinges' are thin pieces of plastic which weigh almost nothing yet are equally as workable as standard aircraft hinges and were used in the first design. Though it was later decided as a last minute design revision to use hinge tape for the elevator assembly to allow for easier assembly.

- Control Sizing

The sizing of elevator and rudder surfaces are estimated using commercial aircraft as frame of reference. The elevator and rudder sizes ranged from 20 – 40 % chord (Saedrey 2013, pg 674, pg 687). Since this aircraft design is flying a relatively slow speed, the decision was to maximise the pitch and yaw control authority. The size of elevator and rudder for the aircraft design are 30% and 35% chord respectively. In the wind tunnel testing phase, the aircraft had adequate pitch control which is a positive result given that it was not analysed in further detail.

Load Path Validation

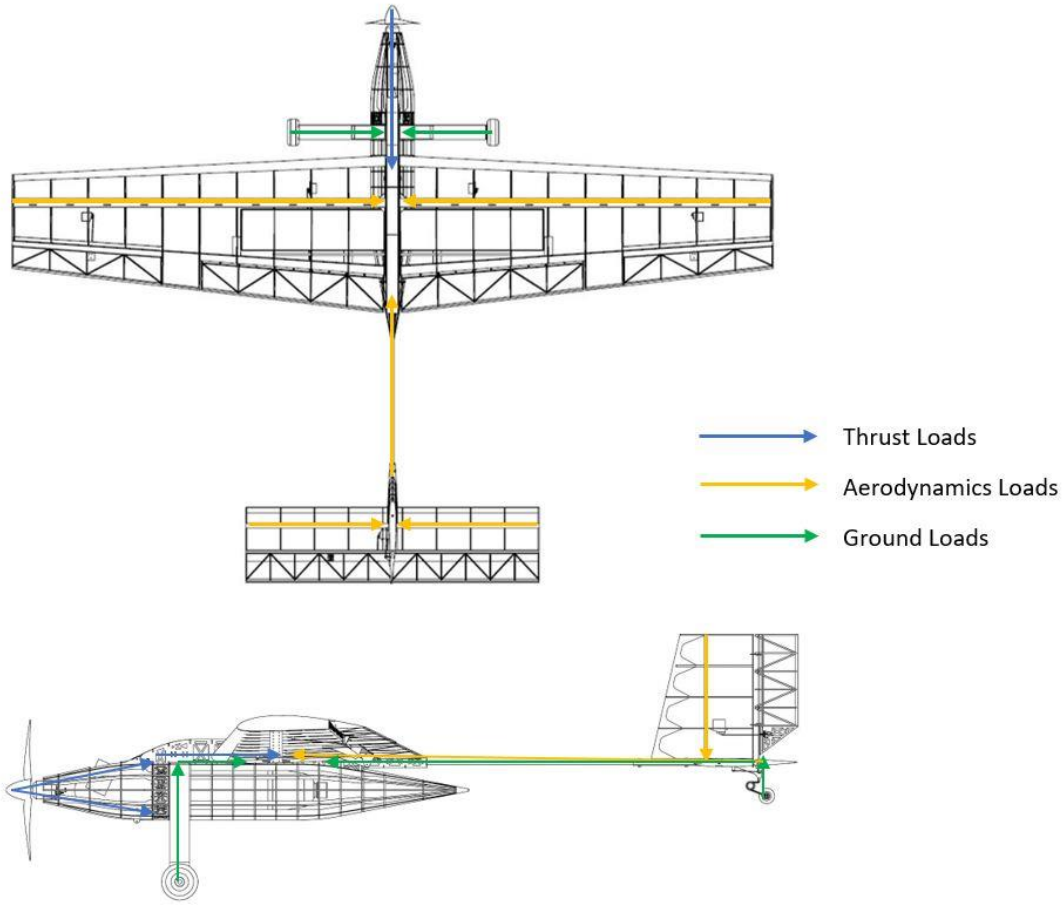

Figure 4.2 Load Path analysis.

As the structural design evolved, it was ensured that all loads could be adequately transmitted to major load bearing elements.

Three types of loads were identified:

1. Thrust loads: motor thrust, torque and vibrations
2. Aerodynamic loads: Wing lift, drag, moments
3. Ground loads: landing impacts

Although the above depicts a fully detailed design, it serves to demonstrate how the load path was analysed at every stage of the design. The evolution of the structure is further discussed in section Fuselage Design Changes in V2. A common feature in all iterations of the fuselage was the two parallel and vertically orientated elements to which all fuselage bulkheads were connected. This serves as an example of how the major load bearing elements were designed first, while all other aerodynamic structures were designed around these primary elements. In so doing, the integrity of the core structure was always maintained.

Payload Receptacle

As per the requirements outlined by the 2018 BMFA weight challenge the UAV must carry a removable tank at only 10% the weight of the liquid payload carried. The tank may not take on any structural load and cannot be exposed aerodynamically. One obvious choice that guaranteed no leaks and the ability to sustain drop tests is a soda bottle. Soda bottles are designed to remain pressurised until consumption, hence the bottles are formed in a way to withstand a degree of stress. The 10% weight issue is not of any concern when purchasing typical bottles of 1.5 – 2L capacity. With these considerations in mind, the primary design challenge revolves around the structures surrounding and securing the payload.

In regard to custom built payload receptacles, one potential strategy was to purchase a flexible water pouch and fitting it within a rigid 'tank' structure that can be removed as a single unit. However, this would be hard to encompass within an aerodynamic shape. A uniquely shaped tank was included in the wings to increase the capability of a higher competition score. The idea was driven forward because it provided the final design with an elegant engineering solution.

4.2 Powertrain Analysis

The power system set by the BMFA competition is the E-flight Power 10 motor, an E-flight 40 amp or a specified equivalent speed controller and, a 3 cell LiPo battery consisting of a 2200Mah capacity. Therefore, the limitations on both the powertrain and power supply, force emphasis in maximising the propeller effectiveness of the aircraft design. To find the most effective propeller for the aircraft, several propellers were tested to gain a greater understanding of how each propeller affected the aircraft, by varying both the diameter and pitch.

The most important requirements of the propeller would be minimising the amount of current drawn whilst in cruise thus increasing the endurance of the aircraft. Furthermore, the propeller must be able to operate at the optimum advance ratio, providing additional thrust for take-off and manoeuvring.

Testing the propellers shown in table 4.1, meant the maximum power was drawn from each propeller thus determining the motor performances. The current, voltage and rpm were measured for each propeller test.

Propeller (inch)	Current (Amps)	Voltage (V)	Power (W)	RPM
11x5.5	29.2	10	290	9000
11x8	32.8	10.6	343	9200
12x6	34.2	9.6	320	7935
12x8	35	9.4	329	9000
15x10	30.7	10.65	327	4572

Table 4.1 Propellers of different diameters and pitch testing results.

In comparison to other propellers, the 12x6 propeller generates a relatively high power to rpm ratio. A finer pitch on the propeller supports the generation of additional thrust. The 12x6 propeller was selected as the P/W ratio was larger than required, therefore generating sufficient power for all rounds of the competition.

Figure A 5 in the Appendix compares C_T, C_P and $\eta 0$ for the 12x6'' propeller. Operating on the linear section of the efficient curve between J-values of 0.4-0.5 would be ideal for the aircraft to operate at the maximum efficiency. J is proportional to the rpm during straight and level flight therefore, excessive rpm can result in an efficiency of 0 and should be avoided. This results in a net thrust of nil which is caused by the air being expelled out into the slipstream at the same velocity as the freestream.

The throttle map for the design aircraft operating at its MTOW is shown in figure A 6, Appendix. A value of 0.48 is found to be the optimum advance ratio to operate at. The peak propulsive efficiency of the aircraft is limited, as the design speed of the aircraft is set at 9-20m/s. After Analysis, the greatest power is required in round 3, where MTOW is the largest. J is approximately 0.47 during S&L flight, where majority of the time the aircraft will be flying. The throttle setting, and propulsion efficiency is 72% and 73% respectively.

Whilst the aircraft banks, J is found to be a value of 0.45, where the maximum throttle setting occurs at 74% and has a propulsion efficiency of 72%. During the propulsion testing of the 12x6 propeller, the maximum throttle setting was achieved hence, the efficiencies are considered satisfactory and demonstrates the selection of the propeller to be appropriate. Furthermore, the total power into the slipstream will pass over the wing as it is positioned at the front of the pod.

4.3 Aerofoil Selection

For the purposes of the BMFA Payload Challenge it is of paramount importance to select the appropriate aerofoil geometry and aircraft configuration. An aerofoil selection criterion is compiled to determine a desirable aerofoil geometry for the payload mission:

- Highest Max. C_L
- Highest Lift to Drag Ratio
- Greatest Lift Curve Slope
- Minimal Pitching moment
- Gentle Stall Characteristic
- Structurally Reinforce-able Aerofoil
- Low AR wing to utilise wing volume for payload storage

Aerofoil Lift Curve Slope

The aerofoils chosen for comparison were the NACA 6514, NACA 4412, NACA 4418 and the 11% thick Clark-Y. Figure A 10, appendix, shows the lift curve slopes of the various aerofoils which for the most part perform similarly relatively to each other. At the shallow angles of attack of around 0-5°, the operating CL ranges around 0.5 to 0.8. Though the NACA 6514 performs weaker compared to the other aerofoils. At zero angle of incidence, the NACA 6514 has less than half the lift coefficient of the other aerofoils which is not an ideal take-off parameter due to the reduced lifting potential. As for the other aerofoils, they are all capable of reaching a C_{Lmax} of approximately 1.35. Though there is some variation in the stall angles. The NACA 4412 and 4418 reach the onset of stall at roughly 11°, however the Clark-Y reaches stall at an AoA of roughly 15°. This makes the Clark-Y a more appropriate choice in climbing steeper angles. Also comparing the Clark-Y to the NACA 4412, the Clark-Y appears to have a more gradual stall, whereas the NACA foil is more severe. For an easy and safe stall recovery, the Clark-Y foil is the more desirable of the two.

Aerofoil Pitching Moments

Figure A 11, appendix, illustrates the pitching moment coefficients of the aerofoils selected for comparison. Ideally the aerofoils should have a minimal pitching moment approaching zero. The larger the pitching moment is, the larger the tail surface has to be to keep the aircraft in balance. The larger tail will also correspond to a heavier aircraft which is certainly undesirable since one of the design goals is to minimise the weight of the aircraft. At low angles of attack, the NACA 6514 serves as the lowest pitching moment. However, post-stall the aerofoil generates a nose-up pitching moment which only serves to propagate the stall, making it a problematic aerofoil to use. The next best profile is the Clark-Y which generally has the lowest Cm-values as well as avoiding the unwelcome post-stall nose-up moment. During the wind tunnel tests, the aircraft was very stable longitudinally; it experienced no drama when the aircraft was pitching up and down. But this can also attributed to developing a well-balanced aircraft.

3D Wing Comparison – Lift to Drag Ratio

Though drag is not the limiting factor of this wing design, it's still important to make as many aerodynamic gains possible given the limited power configuration. Figure A 12, appendix, demonstrates the lift to drag capabilities of the respective aerofoils. Obviously, the intended design should maximise the potential lift to drag ratio of the aircraft. The tangential lines represent L/D_{max} of the respective aerofoils, with the NACA 6514 having the lowest L/D and the NACA 4412 having the greatest L/D, with the Clark-Y very nearly the same value.

When transitioning to 3D analysis of the wing geometry, the maximum lift to drag ratio can be seen more visibly for a variable range of flight conditions. This is illustrated in Figure 4.3.

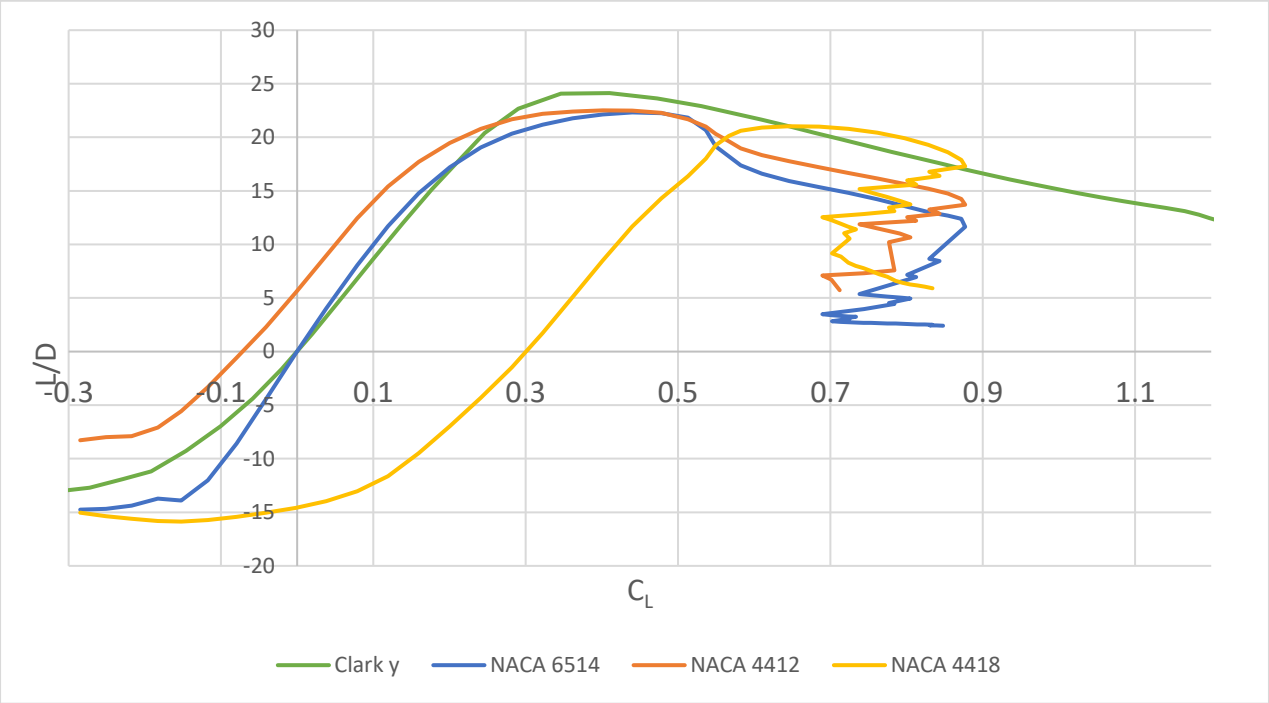

Figure 4.3: Lift to Drag Ratio with variable CL – Airspeed: 15 m/s.

Here the Clark-Y appears to perform the best, with an L/D peaking at 24 with a corresponding C_L value of 0.3. Throughout the cruise segments of the mission profile, the most optimal range of angles of attack should be kept between -1° and 4° to maximise aerodynamic efficiency. And in the interest of efficiency, time spent in the climb segment at higher angles of attack should be minimised. Though the high lift to drag ratio is better maintained at higher angles of attack, since the performance of the aerofoil significantly drops at low or negative angles of attack.

Pressure Drag

It's worth noting in Figure A 13, appendix, that the pressure drag from the NACA 6514 has a significantly smaller pressure drag contribution compared to the other aerofoils. However, that is likely down to the geometry of the profile, there is minimal curvature over the first 50% of the chord, making it more symmetrical in appearance. In contrast, the maximum camber of the other profiles is located closer to the leading edge, resulting in more severe adverse pressure gradients due to the greater aerofoil curvature.

Wing Taper

For the taper, its main purpose is to further lighten the aircraft structure. Looking at the lift distributions in Figure A 14, appendix, it can be seen that as you increase the taper, the peak C_L value begins to shift toward the outboard sections of the wing. The danger of a tip stall is particularly concerning for a highly tapered wing. In a banked turn, the high angle of attack means that the highest CL value occurs at the wing tip. If the tip stalls during a turn, the lift washes out down the rest of the wing which would induce a spin. To keep a balance, we

decided to keep a taper ratio of 0.6 in the main design to lighten without compromising the dynamics of the aircraft.

Given the details of the aerodynamic analysis, the aerofoil selected for the aircraft design was the *Clark-Y profile.*

Wing Twist

Though a parameter which was not investigated was the effects of wing twist. The benefits of introducing wash-out (negative incidence at the wing tips), is that that it reduces the CL value at the outboard sections of the wing. This is especially valuable for tapered wing designs as the smaller tip chord produces a higher CL value locally, and wash-out helps prevent the wing from stalling at the wing tip by reducing the angle of incidence. Though the reason it was not investigated was that it would significantly increase the design complexity of the wing and was therefore not designed for. Though the failure mode of the aircraft during the flight test is something nobody in the design team would've performed any analysis for. The root cause being a differential wing twist. The right-hand wing had a slight wash-in and the left wing had a significant wash-out (which was unintended). The asymmetry in the wings meant that the distance of the respective mean aerodynamic centres from the body were unequal, causing a lateral moment imbalance. The right wing was performing significantly better lift-wise in relation to the left wing. From Figure A 10, we can see at the negative incidence, the CL value approaches zero at approximately -4° which is all it takes to reduce its effectiveness of the wing. And the ailerons were unable to level off the aircraft in response to the roll induced by the inherent wing twist. There was no way to foresee this issue without physical testing and it also indicates intolerance to such aerodynamic dissymmetry. It would be interesting to mount the aircraft on a gimbal, and possibly try to attempt compensation techniques to artificially equalise the lift using the existing features of the aircraft. Possibly differential flaps and ailerons to augment the lift distribution. But of course the resulting secondary effects such as adverse yaw are undesirable and this will also produce unnecessary drag.

4.4 Wing Planform

The wing planform is the shape of the wing when viewed from directly above. A spreadsheet tool was developed to analyse the wing planform for the competition requirements. The template is simplified from Part 2. The wing includes a 60% taper, altering the span-wise load distribution which reduces drag. The outboard loading is also minimised, and this should decrease the wing root bending moment. Tapering the wing increases the likelihood of wing tip stall and the complexity of manufacture. However, the team decided that the skills and time required to implement the added complexity of wing taper was available. The final wing data is shown in the table below.

AR	6
Taper Ratio	0.6
S_{REF} (m^2)	0.661
Span (m)	1.991
Root Chord (m)	0.415
Tip Chord (m)	0.249
MAC (m)	0.339

Table 4.2 Wing specification.

The MAC is located where the construction line interferes with the half chord line. (1) This occurs at 45.8% span. The CG position is initially estimated at 25% MAC but this will shift in each round as the payload is adjusted.

When the wing was designed the leading edge was angled back to allow the half chord (representing the main spar) to attach and sit perpendicular to the fuselage. This decision was implemented for ease of design and manufacture. The wing planform was not updated at the time to replicate this change. Had this been done, the CG position estimate would have been more reliable and therefore less time would have been spent in identifying the CG location. The initial and updated wing planform is shown in Appendix as Fig. A 8 and Fig. A 9 respectively.

4.5 Tail Plane Sizing

The tail plane must be able to trim, provide stability and control the aircraft through elevator deflection. The tail sizing criteria requires the use of the following volume coefficient formulae:

$$V_h = \frac{S_h l_h}{S\bar{c}} \; and \; V_v = \frac{S_v l_v}{Sb}$$

Equation 5 Tail volume coefficients

The volume coefficients used for the equations above are estimated based on those for current aircraft. This should ensure the design can deliver the necessary stability and control characteristics. The volume coefficient is between 0.4-0.7 and 0.07-0.1 for the HTP and VTP respectively. The HTP should provide sufficient pitch control whilst the VTP must offer appropriate yaw stability. The elevator will expand the full length of the horizontal stabiliser at 40% chord. The HTP and VTP have surface area of approximately 23.1% and 17.8% of wing area respectively.

Values l_h and l_v represents the distance between the tail aerodynamic centre and aircraft CG. For simplicity the two were equated at 0.85m. A shorter length would require a larger tail surface area to trim the aircraft. This adds on a significant amount of weight compared to extending the moment arm and reducing the size of the tail plane.

	HTP	VTP
AR	4	2
Taper Ratio	1	0.8
Volume Coefficient	0.58	0.076
S_{REF} (m^2)	0.153	0.118
Span (m)	0.782	0.485
Root Chord (m)	0.195	0.269
Tip Chord (m)	0.195	0.216
MAC (m)	0.195	0.243

Table 4.3 Tail-plane geometry.

4.6 Control Surface Sizing

To aid in aircraft control, several high lift systems were incorporated into the design. These included ailerons, flaps, a rudder and an elevator. For the rudder and elevator sizing, refer to section configuration selection and materials, tail plane. For the flap sizing, an estimate was taken to reflect that of a conventional commercial aircraft. The flap sizing ranged from 25-30% chord. After the decision to include wing tank receptacles, the upper limit of 30% was taken to maximise lift performance during the take-off and landing. The flap span length was taken as 50% of the semi span, reflective of model aircraft. The aileron sizing was calculated using equations 11-15 as shown in the appendix. The sizing of all the flap and aileron control surfaces are illustrated in the table below.

	Span (mm)	Chord (mm)	Area (mm^2)
Flaps	497.20	101.70	50565.24
Aileron	380.00	87.15	33117.00

Table 4.4 Determined chord, span and area for aileron and flap.

The above values, however, were not used during the detail design. The values were not communicated effectively and as a result, during the detail design of the control surfaces, alternative estimates were taken. The initial estimate, seen in V1 for the aileron span was deemed too great and reduced to 85mm. Similar to the first estimate found, shown above. Therefore, time spent in detail design returning the aileron span to a similar size found in the preliminary analysis, could have been avoided.

4.7 Servo Selection

The decision to include high lift systems in the final design required servos for each control surface to be selected. The weight of servos increases linearly with the amount of torque output. The amount of required servo torque also increases with flight speed, refer to appendix, Figure A 7. Weight reduction was a key factor in ensuring a successful score, as proven in the scoring analysis. Therefore, it was important that the correct servos with appropriate torque were chosen. Once the control surface sizing was completed, the amount of torque required for a given deflection could be calculated. The torque was calculated using equation 10, refer to appendix. The deflections were estimated generously to ensure that the servo selected could provide more than enough torque. The calculated torque for all control surfaces are shown in the table below.

	Ailerons	Elevators	Rudder	Flaps
Control Surface Angle, S (°)	30	30	30	33
∠control surface/∠ servo	1	1	1	1
Servo Angle, s (°)	30	30	30	33
Chord, C (mm)	85.0	84.5	82.8	112.0
Span, L (mm)	400.0	775.0	232.0	500.0
Torque (kg.cm)	1.849	3.54	1.02	4.37

Table 4.5 Calculated torque for all control surfaces.

The deflection reached for the flaps in testing was over 30 degrees. The Bb Turnigy 380 max was utilised for the flaps, with a maximum torque of 4.7 kg.cm. The servo selected for the ailerons, elevator and rudder was the Turnigy Tss-9 with a maximum torque of 2.1 kg.cm. The elevator was particularly large and at a 30-degree deflection, the calculated torque was considerably larger than allocated in the final design. However, it was deemed that a 15-degree elevator deflection was sufficient to control the aircraft pitch. This was later verified during wind tunnel testing. The smaller elevator servo allowed 9 grams to be saved in weight. Although small, weight reduction was always a benefit.

4.8 CG Analysis

A scaling method was employed to make an initial CG estimation to ensure all parts were balanced when proceeding to detailed design of the aircraft. This was then used in conjunction with the CG calculated via SolidWorks to compare and validate. AIAA aircraft from previous competitions with similar flight missions and specification were easily accessible and the data was used for scaling weights and CG locations relative to their MAC. Various components were categorised into structural, propulsion, avionics etc. groups. The weights and CG locations were accurately scaled using features that are dependent on the size and location of a component. For example, the wing weight was calculated by using the ratio of wing area to wing weight from an alternative aircraft, for sample calculations refer to Fig A 15 in Appendix. Using the scaling method, the CG of the aircraft empty mass was found

to be 0.433m from the nose. The percentage difference between the SolidWorks value and the scaling method was later found to be 19%. When completing this method, accuracy concerns were present when completing this method, but the result was deemed to be within an acceptable margin.

5 Detailed Design and Manufacturing

5.1 Version 1 – V1

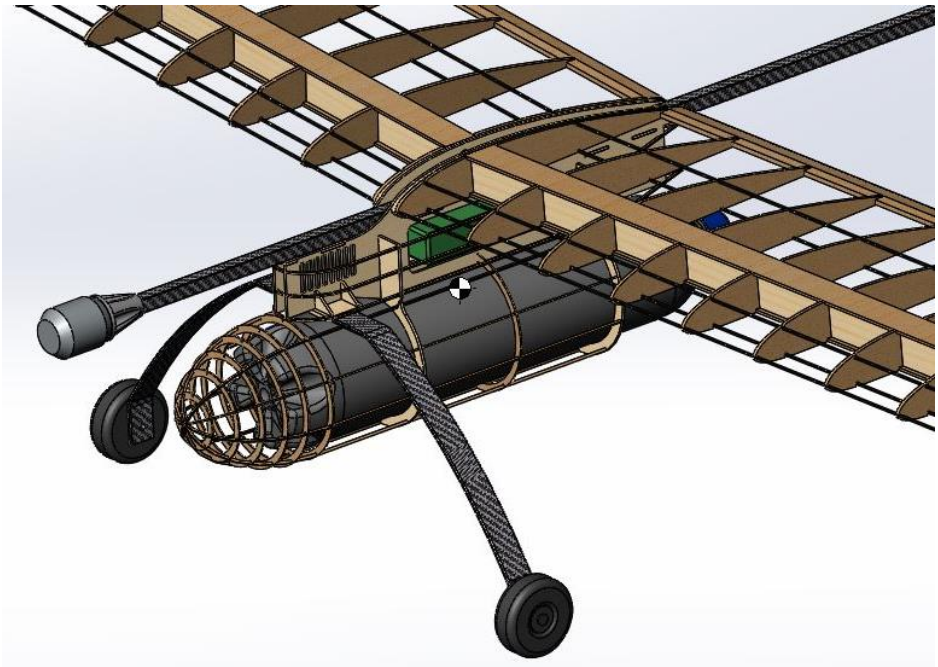

Figure 5.1 Pre-V1 Detailed design.

As envisaged by the preliminary phase the figure above demonstrates the pod and rod concept. A central structure surrounds the carbon rod, connecting the wing and pod assembly while also housing the electronics. This detailed design was produced prior to the finalisation of the conceptual specifications, hence the wings were incorrectly sized. Regardless, the core wing spar structure, dihedral implementation, wing leading edge and core fuselage structure were features that remained within the design iterations to follow.

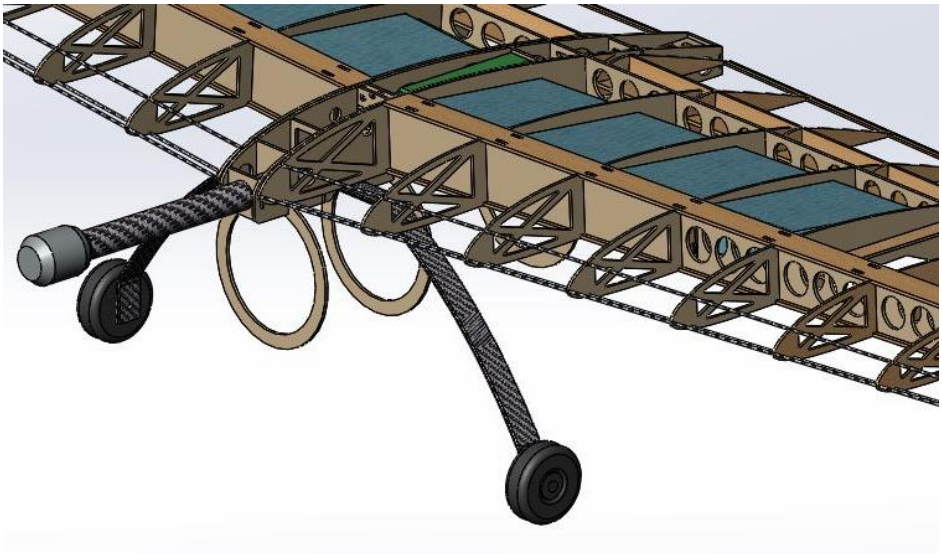

Figure 5.2 V1 detailed design.

Seen above is the first design intended for manufacture, hence V1. At this point in design the specifications were finalised, therefore the wing dihedral, taper and overall dimensions were of the correct size. Due to time constraints, the pod design was incomplete at the time of manufacture, with only the major load bearing elements included. However, these load bearing elements successfully held the full payload during a wing tip test, seen below.

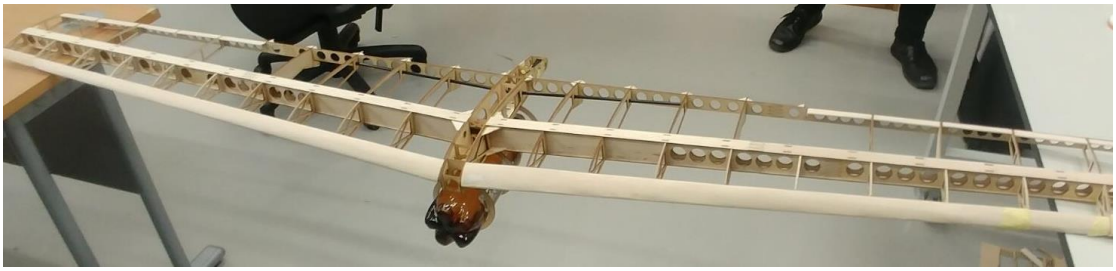

Figure 5.3 Wing tip test.

A few key design changes include; adding more space between the wings to allow the electronics to fit directly between the two removable wings. The 'rod' no longer extends through the full length of the UAV, instead it is broken into two carbon components, one connecting the motor and the other acting as the rear boom. Weight reduction was also applied by removing excess material from the ribs and spar elements within the wing.

The ribs were also split into two elements in the chordwise direction, in other words the rib did not intersect the main spar. Instead the leading edge and central wing box spar element was simply glued onto the vertical surface of the spar. This was a poor design choice as the ribs transferred any aerodynamic or internal load to the main spar via a surface to surface glue joint and nothing more. Further to this, in the manufacturing process of the V1 wing, several ribs were easily detached. This further highlighted the requirement of the wings being modified.

5.2 Version 2 – V2

The final iteration of design saw many improvements, weight reductions and entirely new features, seen below.

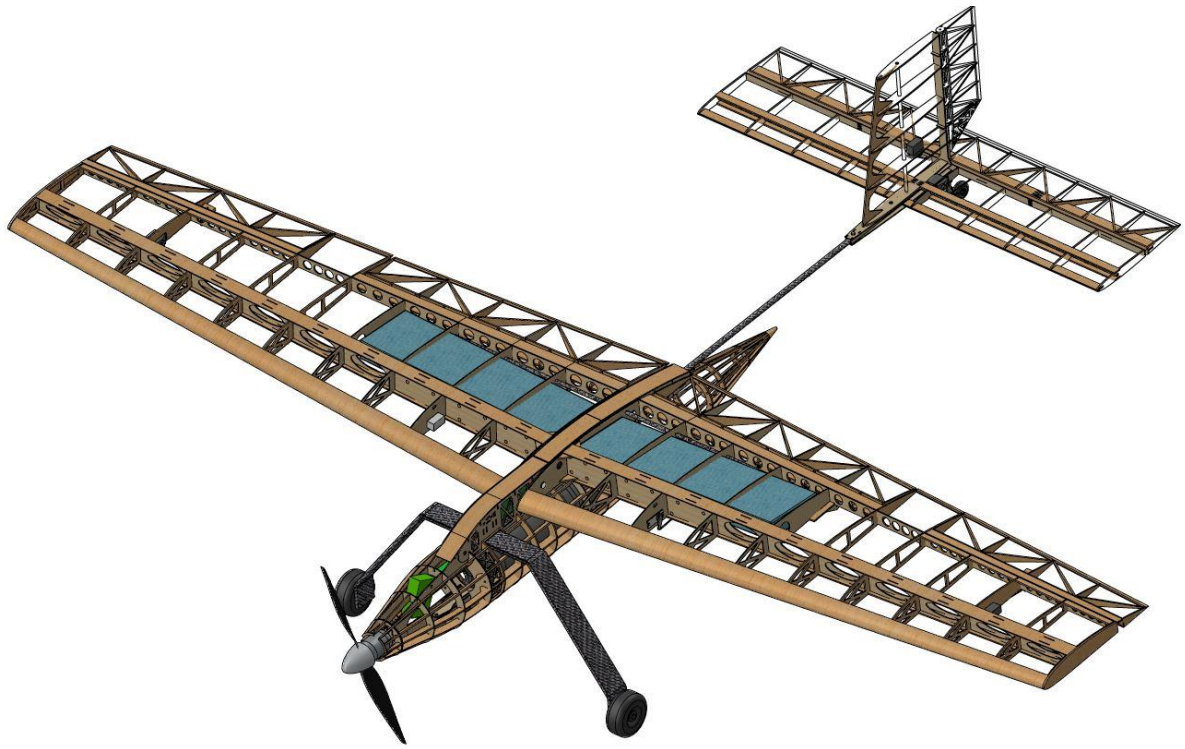

Figure 5.4 Final Design.

The following figures depict the major aircraft components

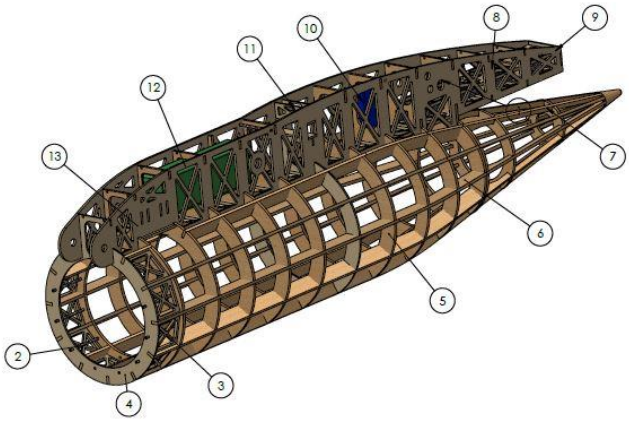

Item No.	Component	Description	QTY.
1	Main Longitudinal element	2mm Plywood	2
2	2mm carbon	Allows for torque transfer to from power train to fuselage	6
3	Torsion reinforcement	1.5mm plywood	10
4	Plywood bulkhead	1.5mm plywood	2
5	Balsa bulkhead	2.5mm balsa	9
6	Longitudinal pod element	2.5mm balsa, slots into bulkheads	11
7	Trailing edge assembly	2.5mm Balsa build up	1
8	Square carbon tube	10x10mm, tailboom insert	1
9	Body Torsion reinforcement	Increases torsional rigidity	15
10	Receiver	Radio Receiver	1
11	Main spar brace	Distributes loads from main spar into fuselage	1
12	Battery	2200mAh 3C Lipo: Overlander Supersport Pro	1
13	Undercarriage hardpoint	Where undercarriage is mounted	1

Figure 5.5 Fuselage assembly.

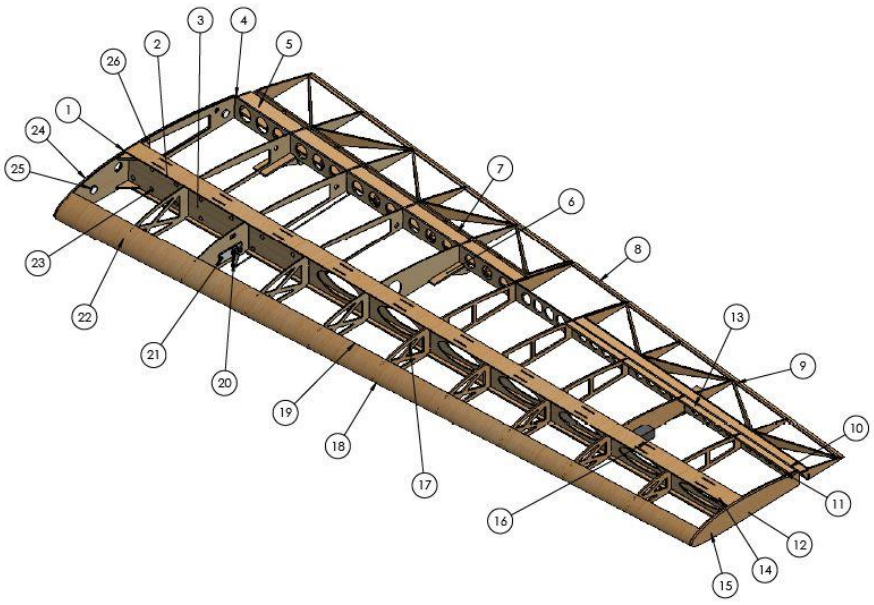

Item No.	Component	Description	QTY
1	Horizontal Spar element	2.5mm balsa	1
2	Wedge Insert	Solid balsa wedge enforcing 3 degrees diherdal	1
3	Wedge liner	0.8mm plywood slip cover	2
4	Flap cover web	Balsa, fills void left by flap leading edge	6
5	Flap Assembly	2.5mm balsa, with 2mm plywood on hinged ribs	1
6	Panel work	Enforces aerofoil geometry around flap hinges	4
7	Flap cover	0.8mm balsa, enforces aerofoil shape	1
8	Trailing edge	Between the flap and aileron	1
9	Aileron Assembly	2.5mm balsa construction	1
10	Aileron hinge mount	Provides a surface for wrapping and as a hinge point for the aileron	1
11	Rear Spar	1.5mm plywood	1
12	Wing end plate	3mm balsa	1
13	Control horn	Mounted to Aileron	1
14	Vertical Spar element	1.5mm plywood	2
15	Balsa Rib	2.5mm balsa slotted into vertical spar elements	6
16	Aileron Servo	Turnigy TSS-9	1
17	Horizontal Spar element	2.5mm balsa	1
18	Carbon stringers	2mm OD hollow carbon embedded into leading edge of ribs	3
19	Leading edge	0.8mm balsa formed over ribs	1
20	Servo arm	20mm Servo arm	1
21	Flap Servo	Turnigy 380Max	1
22	Plywood Rib	1.5mm plywood	5
23	6mm Dowel	Attaches web to spar	13
24	Root plate	2mm plywood	1
25	Wing locking nut	Prevents the wing sliding off	2
26	Root reinforcement	Balsa	4

Figure 5.6 Wing assembly.

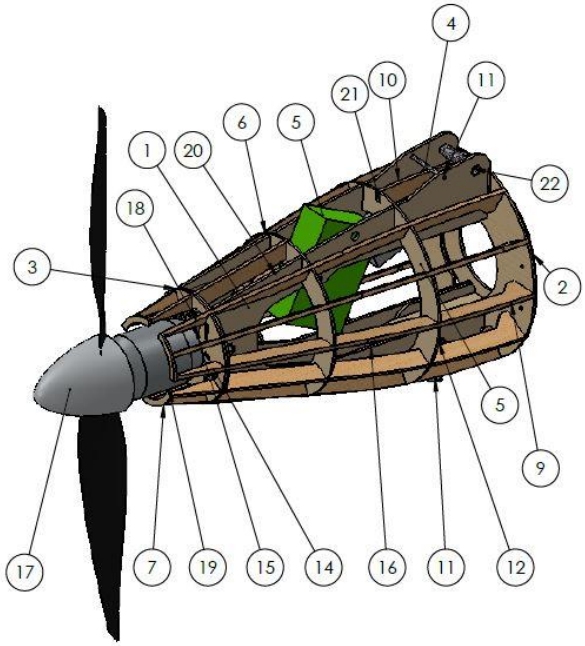

ITEM NO.	PART NUMBER	DESCRIPTION	QTY.
1	Main longitudinal bulkhead	2mm plywood	2
2	Bottle stopper	1.5mm plywood	1
3	Firewall	1.5mm plywood	2
4	Bulkhead 1	1.5mm plywood	1
5	Bulkhead 2	1.5mm plywood	1
6	Bulkhead 3	1.5mm plywood	1
7	Nose leading edge	1.5mm plywood	1
9	Longitudinal element	2.5mm balsa	7
10	Longitudinal element 2	2.5mm balsa upper element	1
11	2mm carbon 30mm	Serves as push point for latch	2
12	5mm carbon 32mm	Axis for latch mechanism	1
14	M3 Bolt	Steel	6
15	M3 Nut	Lock nuts	6
16	Latch Assembly	Plywood assembly, locks nosecone in closed position	1
17	12x6 Prop	-	1
18	Motor mount	-	1
19	EFlight Power 10 Motor	-	1
20	Fuse holder and fuse	-	1
21	Speed Controller	Eflight 40amp Speed controller	1
22	6mm carbon hinge	Axis for nosecone rotation	1

Figure 5.7 Nosecone assembly.

5.3 Design Changes V1 to V2

Fuselage

The V1 design was found to be severely tail heavy when fully loaded, therefore the structure was essentially extended forward. This enabled the shifting of the battery ahead of the main spar and the forward shifting of the landing gear. This allowed the CG to be balanced for all three rounds.

The bulkhead elements forming the pod structure were spaced linearly at 40mm spacing down the full length of the fuselage. This change increased the number of bulkheads to 11 instead of the previous 3. Initially these elements were all designed as 1.5mm plywood, however since it was previously proven to hold the 1.5kg payload with only 3 bulkheads, these elements were downgraded to balsa to save weight, except for the bulkhead below the CG and the hinge point of the nose cone. The carbon boom was lose in the rear section of the fuselage in the V1 design. This was effectively removed by adding more bulkheads as the square carbon element extended through 5 bulkheads instead of the previous 3. The manufacture of the V1 fuselage revealed a torsional weakness, therefore in this design diagonal elements were added within each subsection of the fuselage in all planes. This improved the stiffness of the fuselage by a noticeable factor. Finally, longitudinal balsa elements were slotted into the bulkheads at 30-degree intervals, further increasing fuselage stiffness.

From the above figures it can clearly be seen that the forward motor mount was abandoned, and the motor was mounted on the nose cone assembly. This effectively lowered the propeller position and as such the landing gear vertical clearance was increased. The idea was to increase propeller efficiency by removing the effects of a pod immediately behind the outer radius of the propeller.

When designing the nose cone, two vertical and parallel plywood elements formed the major load bearing elements, to which the round balsa structure was attached.

Wings

The final wing design was driven by the need to remove excess weight as the V1 wing was 30% over weight. This was done by reducing all plywood elements from 2mm to 1.5mm. This includes all vertical elements in all main and rear spar in addition to the plywood ribs supporting the weight of the wing tank.

In the previous design, the wing was attached to the fuselage by extending a square carbon element into the internal volume of the main spar. To enforce the dihedral a series of hollow plywood wedges were inserted and glued inside the spar to fill the void and ensure the correct angle. Once again, the major flaw with this design was that it relied purely on glue that was in shear loading. To correct this design flaw and reduce weight, the internal wedges were

downgraded to solid balsa while also being secured to the vertical spar by a series of dowel pins.

Another design flaw addressed in the final version was the chord-wise split of the ribs. The ribs were redesigned to slot into the main spar as once piece. This required adding a slot to both the vertical spar element and ribs, hence reducing the effective thickness of the material. These slots were added above and below in sequence to help reduce the negative effects of reducing the vertical thickness. Finally, the series circular holes added to the vertical spar was modified to a single ellipse between each rib. This effectively removed slightly more material hence reducing weight.

It is interesting to observe the way the UAV design gradually iterated away from the original pod and rod concept. Instead this UAV design more closely resembles a conventional configuration, only in the absence of a full rearward fuselage structure. Perhaps this suggests more time should have been spent evaluating the suitability of each configuration.

Control Surfaces: Flaps

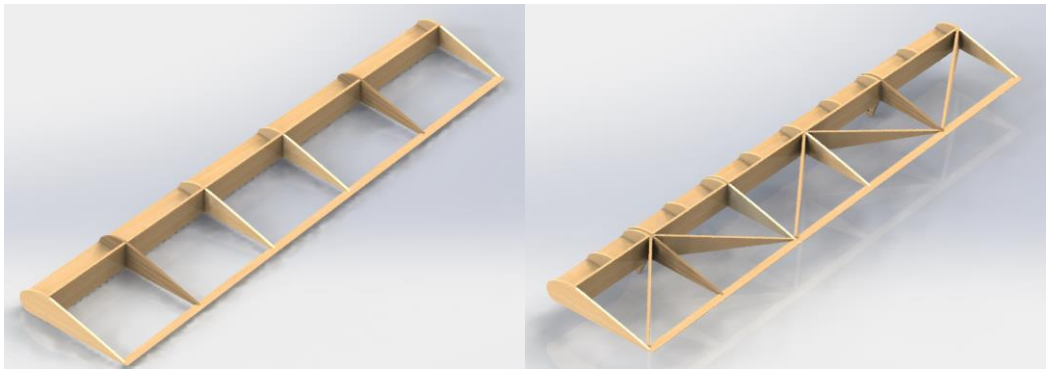

Figure 5.8: Comparison of V1 flaps design (left) and V2 flaps design (right).

The V1 flap reinforcement elements were manually cut and placed horizontally across the top surface in a truss like structure. When undergoing torsion testing, the V1 flaps lacked a resistance to twist. This led to the reinforcement elements, rotated 90° and instead placed vertically. The reinforcement elements were carefully designed to fit the diagonal spacing between the ribs. This ensured the structure did not become warped or twisted.

5.4 Tail Plane

Figure 5.9: V1 (left) and V2 (right) Tail plane Assembly's.

Overall Design Progression

Figure 5.9 illustrates the design progression of the tail subassemblies. From the manufacturing of the first iteration of the design was evidently a failure. This partly stems from incomplete CAD work with to meet the manufacturing deadline but also a laziness in the design itself. Many components in the assembly were simply held by glue joinery. A lack of foresight on the designer's behalf; overestimating the strength of the glue joints. Applying small loads would simply cause the components to shear off. The following iteration capitalised on taking advantage of the potential of the laser cutter to implement some more intricate joins that jigsaw together and provide more mechanical leverage. Additionally, all the 2mm ply was replaced with 1.5mm ply for weight reduction.

Control Surface Design

The control surfaces were particularly challenging to design due to their inherent high aspect ratio and small thickness to chord ratio. To combat this, the design philosophy of the ailerons and flaps were utilised. The composition of vertical elements forming a truss structure served to solve the tendency to bend and twist. A couple of changes were also implemented, namely combining the elevator from a 2-piece to a single piece elevator. The main reason being is to simplify the control actuation necessary to deflect that particular surface. Also the rudder hinging method changed from the flexi-hinge to being hinged on a 2mm carbon tube. The design intention being to connect the tail gear to the rudder hinge line, allowing the aircraft to taxi itself using the rudder servo. The ability to steer the aircraft on the ground run would provide the pilot more control in event of any deviation from the intended flight path. Though the ground run on the flight test was very short, and the aircraft took to the air very rapidly, so its necessity was fairly short-lived.

Spar Design

The main spar of the HTP and VTP in the first design composed of a pair of 2mm carbon tubes, but was flawed in the sense of its distinct lack of rigidity in bending. The intention of the 2mm carbon tube was to maintain a very lightweight structure. However it contributed no

resistance to bending loads, rendering the tail surface useless. The rigidity of a structure generally comes from its second moment of inertia; so the decision was to increase the cross-sectional area. The diameter of the tube increased from 2mm to 5mm and a pair of balsa flanges were implemented to permit additional bending resistance. Also the effect of gluing the 5mm carbon tube into the structure gave the tail surface more torsional resistance along its span.

Central Structure

The central structure changed significantly in design from the 1st to the 2nd iteration. The concept of the first version of the tail plane was to implement a 0.8mm plywood sleeve to wrap around the carbon, secured by a bolt at the end. However, the plywood sleeve was under designed, as it simply consisted of 4 plywood strips glued together. Additionally the 0.8mm plywood was extremely flexible and was an undesirable feature for the tail. So the following design iteration replaced the 0.8mm ply sleeve with a 1.5mm jig-sawed ply box which connected all the components to the central piece. This includes: the spar, the leading edge, the rear spar connecting in and through the box as a single unit. The tail took a few knocks on the flight test which is enough to deem the overall structure as suitable.

Boom Design

One facet of the tail design that was seemingly overlooked was the design of the boom. Originally it was simply an 8mm carbon tube extending out the back of the aircraft bolted into the tail. After the manufacturing and assembly of the aircraft, it was discovered that there was an excessive tail wobble in the structure. This was down to two reasons: the first being that the pultruded carbon tube was not sufficient in resisting torsional loads and the second being the small outer tube diameter. It was difficult to determine the adequacy of the design without running a structural analysis for the validation of the structure. If a woven carbon fibre tube with a larger diameter was used, perhaps this wobble could've been mitigated. Some attempts were made to rectify the problem which involved permanently gluing the tail into the boom to secure the carbon firmly in location. However this did not solve the problem as it does not improve the rigidity along its length. Extra carbon with struts were added and helped alleviate some of the problem. But this highlights the fundamental flaw with the pod and rod scheme. In hindsight, it was probably better to create a dedicated structure to integrate the tail into the main body of the aircraft.

5.5 Wing Payload Receptacle

The polypropylene plastic was finalised as an appropriate material to laser-cut and fold into the main body of the tank in the preliminary design process. The tank was designed to fit through cut out sections in the first 4 ribs of the wing. The lid was designed to be a means of easily refilling and emptying the water tank whilst also being lightweight and water tight. To

ensure the glue used in fixing the tank and lid together would yield the best result for bonding and no leaks, the lid needed to also be made of polypropylene material.

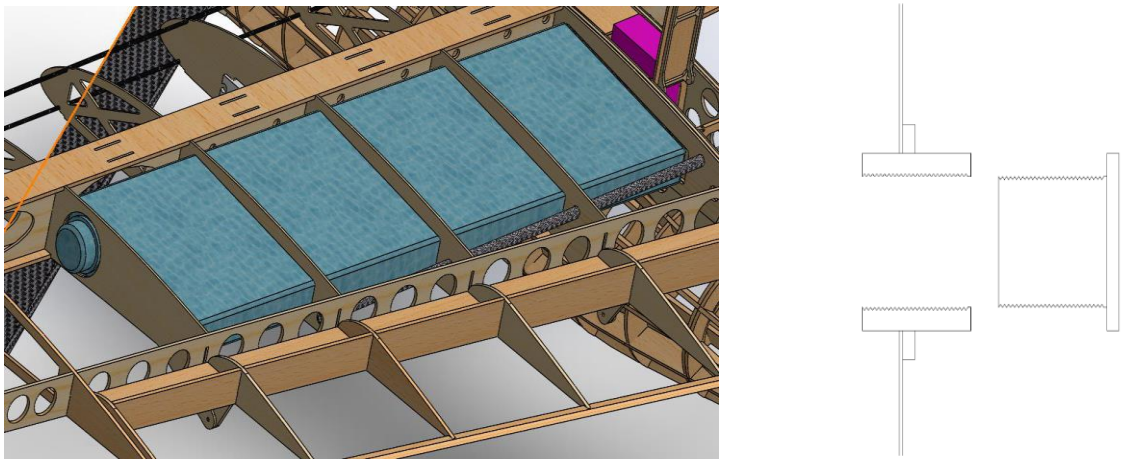

Figure 5.10 CAD design of wing tank (left) and lid (right).

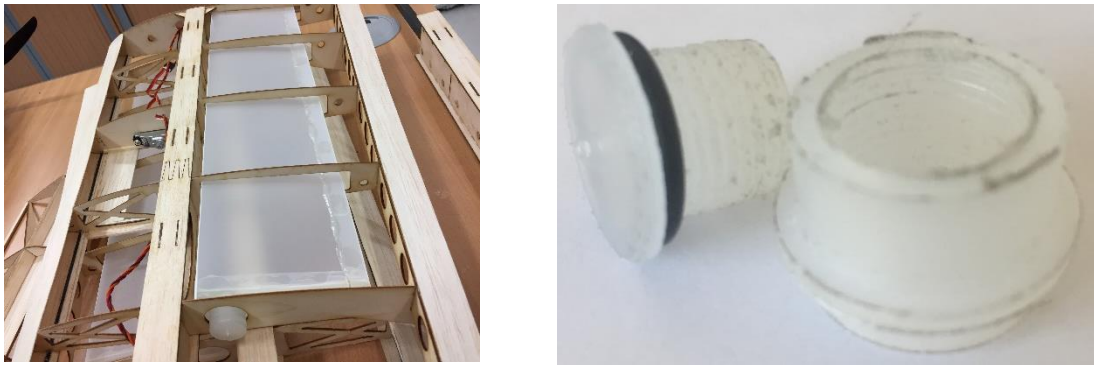

Figure 5.11 Manufactured wing tank (left) and lid (right).

Polypropylene sheet of thickness 0.5mm was laser cut and folded to form the main body of the tank. The material was selected as it was assumed to be structurally rigid and able to keep its shape when filled with water, all whilst being light weight. Polypropylene glue – Tecbond 261 was used to glue the wing tank together whilst also making the joints and edges water-tight. The complete lid section was made of 2 parts, the neck and the screw-in lid. They were both made from a polypropylene rod by machine cutting on a lathe. The neck was hollowed out and tapped on the inside walls to allow for the lid to be screwed in. The neck also has a flange which acts as the contact piece used for gluing to the water tank walls. The lid has the tap on the surface and a rubber O-ring to ensure no leaks occurred once the lid was fully closed.

Although the wing tanks were able to carry the required load of water whilst being watertight, unforeseen issues occurred such as ballooning when filling up the tanks, making them more difficult to fit inside the wing. More iterations were required to make the wing tanks hold its

shape to allow for easy filling up and to ensure no leaks/ cracks in the glue would form overtime. However, the time constraints did not allow for more design iterations and therefore selecting a pre-made tank may have been a better option.

5.6 Battery/Payload removal and installation

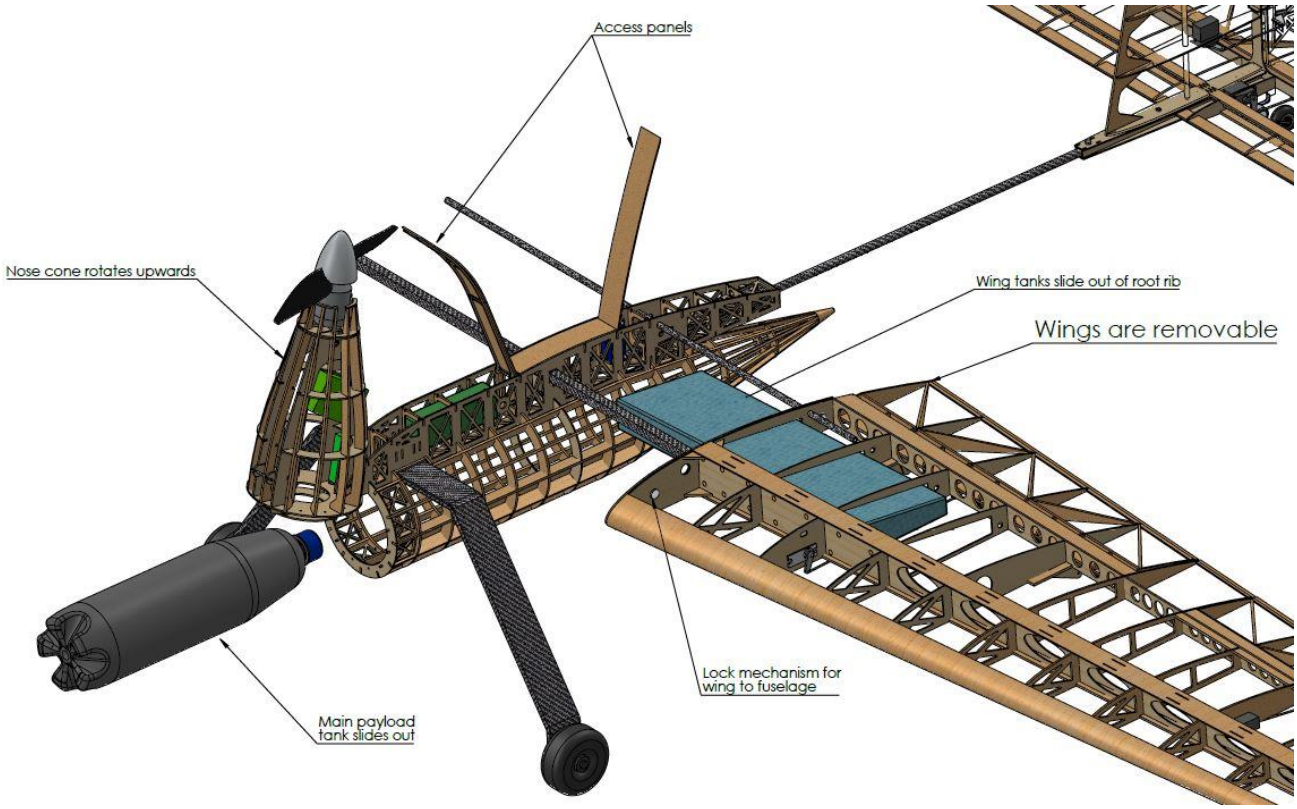

Figure 5.12 Accessibility of battery and payload.

As seen in the above figure, the main payload tank is removed by unlatching the nosecone which rotates upwards. The main water tank fits snug within the pod assembly and once the nose cone is locked into position the bottle is also fixed in place. In a similar fashion, the wing tanks fit snug within the ribs. Once the wings are fully secured to the fuselage, the wing tanks have no excess space to move thus are locked in place.

To the rear and front end of the central fuselage structure, two access panels can be seen open. These access panels give full access to the RC receiver, wing securing nuts and the battery. The space allocated for the battery allows for longitudinal movement only, this enables on the fly longitudinal balancing if needed. Velcro secures the battery within the fuselage enclosure.

5.7 Manufacture

Key assembly tasks

Prior to the main assembly tasks, it must be highlighted that great precision was required to ensure all laser cut pieces fit together exactly as intended. In more detail, when laser cutting

different materials at various thicknesses, the laser feed rate and intensity must be adjusted accordingly. This results in slight dimensional tolerance differences. To gauge and adjust for these tolerances, a series of test pieces were laser cut and physically assessed for correct fitting. This technique was applied to critical finger joints along the main wing spar and fuselage bulkheads.

The need for custom assembly jigs was identified early during manufacturing stages. These jigs were designed to assist in the gluing of components whereby exact angles were difficult to gauge or where extra hands would be necessary to do the job correctly. For example, spacers of precise length and angle were laser cut to assist in the gluing of main structural elements in addition to jigs physically holding components in place to allow for the full use of both hands while applying adhesive.

Post fabrication of all laser cut components, the assembly process began by sorting all components and assembling the structure in the absence of adhesives.

Wing Assembly

Due to maximum laser cutting dimension of 740mm, the longitudinal components were cut as two components and joined together using balsa cement and a series of finger joints. The ribs were slotted within the spar as described by the detailed design and glued in place using a series of jigs.

When assembling the dihedral wedges embedded within the spar, each wedge was made up of 4 sheets of 2.5mm balsa sandwiched together. The dowel pins were cut to length and fitted within the wedges. All contact surfaces were then coated with a layer of balsa cement and fitted in place within the spar. While the wedge inserts were curing in place the carbon spar was repeatedly inserted and removed from the wing spar to ensure it cured with enough clearance for easy wing removal.

Aside from attaching all other components using balsa cement, many extra panels of balsa were added to provide additional surfaces for the final wrap to adhere to. This includes the panel work around the servo access panels and around the flap hinges extending outside the surface of the wing. The final wrapping process required the priming of all wrap contact surfaces with Balsa lock. After the surface was primed the wrap was ironed onto the wing and a heat gun was used to tighten any loose areas.

Overall the process of manufacturing the wings was the most difficult aspect of manufacture. However due to the consistent effort during the prototyping period, multiple wings were built providing the team the opportunity to learn from previous mistakes and to general improve manufacture skill. It must be stated that the complexity of the wing design was a major contributing factor to the difficulty and eventual errors made. With the experience, time and

resources available the team believes that the quality and complexity of the result was above and beyond original expectations.

Fuselage Assembly

The fuselage structure was comprised of three separately assembled components: the central structure, nose cone and tail cone, which were later joined. The following three paragraphs outlines the key tasks for each component respectively.

The main plywood element within the fuselage was anchored to the table using several clamps and all 11 bulkheads were glued into their respective locations. After the second main plywood element was secured, all longitudinal components were slotted into the bulkheads. Lastly, torsional reinforcement members were added throughout the structure. This completed the central structure assembly.

The nose cone was constructed in a similar fashion to the central structure. The central plywood structure was assembled and glued using a series of jigs to ensure straight and true assembly. After this section was cured the circular balsa bulkheads and longitudinal elements were then inserted into their respective slots and glued in place. The latch mechanism was assembled separately and later installed into the nose cone. The motor mount and fuse holder were bolted in place prior to any wrapping of the outer surface.

The tail section of the fuselage was assembled separately using a specially designed jig to position the bulkheads in place prior to inserting the 12 longitudinal elements forming the cone shaped section.

In hindsight the fuselage structure was not particularly difficult to manufacture due to the straight and square nature of all interlocking elements. Small challenges presented themselves along the way, such as inserting the longitudinal elements into the bulkheads, however overall result was exactly as intended. In terms of manufacture, this process was a fantastic example of a structure designed with the full manufacture cycle in mind.

Tail plane Assembly

Like the main wing assembly, the core structure intended to slide onto the carbon boom was assembled and glued first. To which the main carbon spar elements and rear plywood elements for the tail plane were inserted and glued in place. Beyond this stage it was a simple matter of sliding the appropriate ribs onto the carbon spars, followed by slotting them into place on the rear spar. Once each rib was ensured to be straight and true they were glued in place, followed by the leading edge of the horizontal/vertical stabiliser.

Included in the tail plane assembly was a steerable tail dragger wheel. The steering axis that enabled steering was aligned with the rotational axis of the rudder, and as such the two axis materials were connected to enable torque transfer from the rudder to the wheel. The issue was that the material used as the rudder axis was 2mm hollow carbon tube. The torsional flex of this material meant that even with full rudder deflection and a perfect connection the

wheel would not steer as intended.

Figure 5.13 Rear steering fix.

The above figure displays the use of a zip tie, nut and bolt and wheel collet clamping the two elements together at the lowest point of the rudder.

To reflect, the tail plane manufacture of the final iteration was significantly easier than the original. This is largely due to the effort put into the interlocking of all components, reducing the margin for alignment error and incorrect component placement. However still present in the final stages was the unnecessary complexity of the rudder and hinge mechanism, whereby the axis intersected with the motion of the elevator. This required extra trouble shooting to rectify as illustrated above. Aside from simplifying the design, one major improvement to the manufacture phase would be the inclusion of extra wrapping surfaces near the internal corners of the tail plane. This would provide sufficient adhesive surface area to easily wrap these features.

Control Surface Assembly

All control surfaces, including the flaps, followed the same assembly process due to the similar design. Essentially each control surface was designed to include a vertical and horizontal spar element to form a type of L bar. To which the ribs and diagonals were slotted and glued. Due to the virtual assembly process within SolidWorks the dimensions and overall fit of each component was validated. Therefore, when assembling the control surfaces, by fully inserting all components into one another the control surface was guaranteed to be straight and true. Due to warping of the control surface over time due to glue contraction, special care was taken in later iterations by placing weights along the length of the spar to ensure straight curing.

By the end of this project, collectively over 20 individual control surfaces were manufactured. This process allowed for significant design refinement and manufacturing quality. The only improvement that could be made is investigating the absolute exact laser cutting tolerance to avoid the gradual warping due to glue contraction.

6 Testing

6.1 Wing Spar

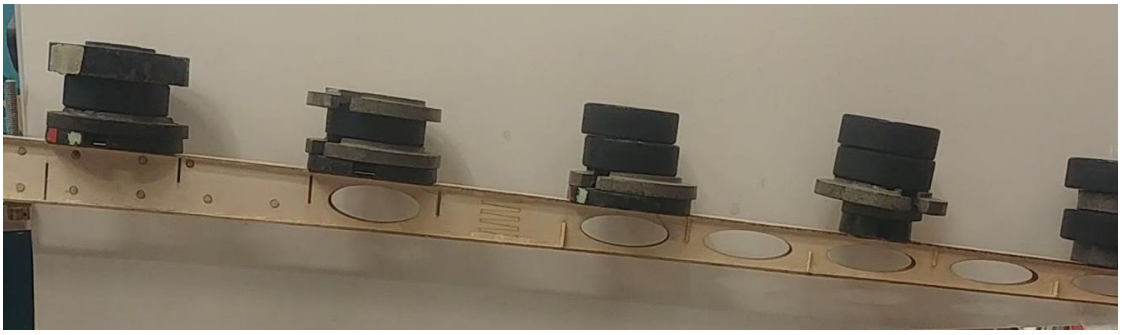

Figure 6.1 Wing Spar at 7.16kg loading.

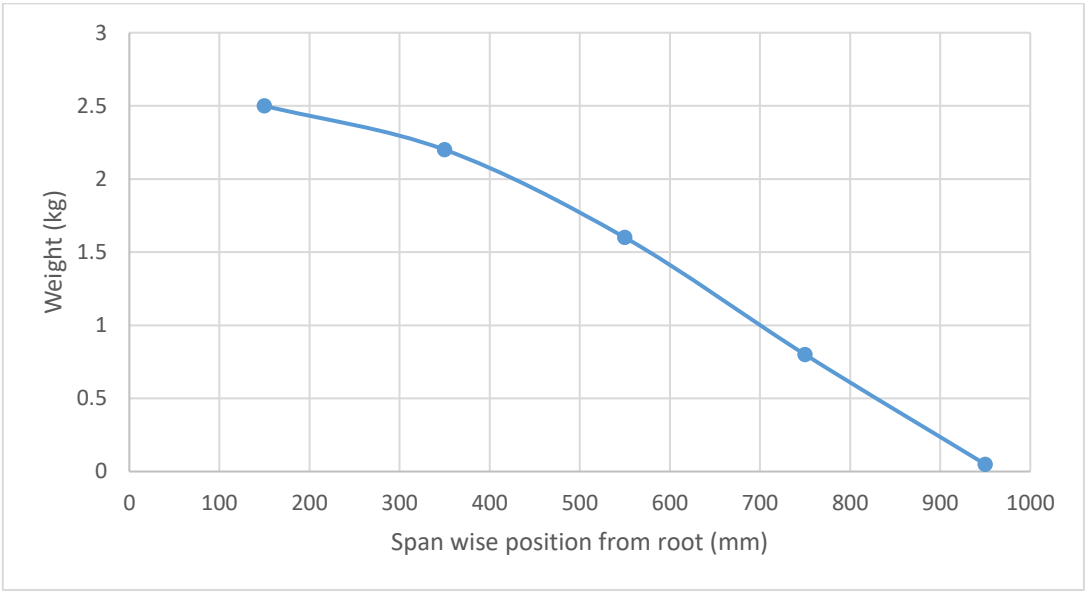

Figure 6.2 Load distribution at Failure.

After the final design was complete, a test spar was manufactured to specification for the intention of ascertaining the loaded failure point. The spar was clamped upside down to a table by the carbon spar extending from the root and small weights ranging from 150g to 500g were added gradually until failure. Placeholder pieces of balsa were also glued into the voids left by the rib slots (this is visible in the above figure). The image above displays the spar immediately before failure and the corresponding load distribution. A total of 7.16 kg was applied at which a maximum deflection of 95mm was recorded at the tip. This represents a safety factor of approximately 2.4 when considering maximum payload flight, hence validated the strength of the main spar.

6.2 Wind Tunnel

Figure 6.3 Wind tunnel test set up.

After full assembly, linkage and visually guided trimming of all control surfaces the UAV was suspended by the wing tip spar location within the wind tunnel on campus. The primary purpose of this test was to establish the longitudinal stability during cruise conditions. The secondary purpose of this test was to validate the flap deployment, while also paying close attention to any secondary motion induced while deploying the flaps.

Two separate rounds of tests were conducted, both displaying highly sensitive pitch control and stable flap deployment, essentially validating the longitudinal stability. During the manufacture phase the boom flex was of concern, however the wind tunnel 'flight tests' revealed that the propeller wash over the tail did produce a slight vibration, however it was concluded that the observed tail vibration was below an acceptable level.

6.3 Flight Test, Bedfordshire

To validate the flight capability of the UAV a test flight was conducted in Bedfordshire. With the knowledge of acceptable pitch control and CG position it was assumed that the UAV would fly smoothly. During the first flight, on take-off rotation the UAV performed an uncontrolled roll, left wing down. Luckily the pilot managed bring the wings back to a level position before touching down hard into long grass. This impact tore the landing gear from the fuselage mount. The repair involved inserting a block of balsa beneath the landing gear, fixing the landing gear in place. It was assumed that the aileron deflection was insufficient to cancel out the aerodynamic effects causing the anticlockwise role. Therefore, the maximum deflection angle was increased by adjusting the servo linkages.

During the second test flight, the same uncontrolled left-wing role occurred. However, the pilot committed to the take-off, at which point the role continued and the left-wing tip

impacted the ground, resulting in the somersaulting of the UAV and several other impacts on the nose cone and tail plane. The impact on the nose cone caused the complete catastrophic separation of the nose cone from the fuselage.

It was concluded that the uncontrolled roll experienced in both flights was the result of lift asymmetry within the main wing, caused by unintentional wing twist. This wing twist was the result of manufacturing errors. In more detail, the plywood used in main vertical spar was significantly warped before manufacture. During the curing of the spar no clamping or weights were utilised to ensure the spar was straight and true. Therefore, as the glue cured, the internal stresses generated by the warped material generated a slight twist over the span of the wing.

7 Project Review

7.1 Technical Review

The ETM071 MEng Aeronautical Design Project aim was to exploit previous engineering knowledge to design and build a working air vehicle. In the 1st term, the aim was to complete a conceptual and preliminary design for the AIAA DBF. A payload and MTOW configuration was determined as a result of a thorough conceptual design and scoring analysis. This was later discovered to be similar to the design which went on to win the AIAA DBF 2017/2018 competition. In the 2nd term, the team incorporated build and test phases into the design process for entry to the BMFA 2018 competition. The project vastly encompassed skills learnt in the past three years of study, specifically those learnt in part 2 Aeronautical Design and Analysis. In the 1st term, the conceptual design proved lengthy as the majority of tools and skills required were unused since part 2. However, the time spent proved to be valuable.

In the 2nd term, team members were confident in completing the conceptual phase independently as a lot less guidance was required. This lead to the conceptual and preliminary design phases being completed in under 2 months for the BMFA. Further to this, preliminary design was covered loosely in previous years so output quality was basic in the 1st term and this was noted moving forward. The preliminary design phase for the BMFA was more thought out and greater effort was put in to understanding values found in the aerodynamic analysis and empennage sizing. However, the aerodynamic analysis was not perfected, and detrimental effects of twist was overlooked. This was because a large focus was placed on longitudinal stability rather than lateral stability. This was later translated into manufacturing and proved to be fatal during the flight test. Other challenges in the design process was finding a trade-off, agreed by all team members, between structural integrity and a low aircraft empty mass. This was the key technical objective to being successful in the competition. After manufacturing the first iteration, the wings were found to be 30%

overweight without the inclusion of electronics. This resulted in two full iterations being completed with the main aim to reduce component weight in the wings.

The desired output was to design and build an unmanned air vehicle that can safely carry the payload and aircraft empty mass prescribed in conceptual design of 3.5kg and 1.74kg respectively. The aircraft empty mass of the final design in SolidWorks was found to be 1.7kg. The aircraft empty mass of the final manufactured design came to 2.08kg, i.e. 34% overweight in reference to higher value. This value greatly exceeded the 20% limit imposed. However, both these values excluded the weight of the electronic cables, wrap and glue. The lack in manufacturing experience in the team also did not help. The maximum payload to aircraft empty mass ratio that could have been achieved was 1.68. This would have produced a score of 134.4 in the final round of the BMFA 2018 competition, potentially placing Aquarius in 3rd place.

One of the main risks in the project was the lack of time to complete a ground and flight test before the competition. This left questions about the controllability of the aircraft during flight. Although a CG and stability analysis was performed, these analyses were simplified and thus the accuracy was questionable, at best. The final design had veered towards a low aircraft empty mass and was not built with reparability as a priority. Furthermore, the intricacy of the design meant a small component failure could not be instantly repaired instead, the entire component would require replacement. For example, failed ribs would result in the wing being replaced.

A flight test was completed the day of the competition. A negative twist on the wing shifted the aerodynamic centre to the left producing a lift imbalance in the wing. This resulted in the aircraft crashing and the fuselage sustained considerable damage. The design currently remains in progress, the left wing will be completely rebuilt, and adjustments will be made to strengthen the fuselage. The lack in manufacturing precision proved critical and in the aftermath of the crash, all team members will be sure to not make such a mistake again.

7.2 Managerial Review

The main issue in the design project was the management of time. The unavailability of the BMFA competition specification from the offset left one term for the entire design process to be completed. The original timeline allocated the 1st term for the conceptual to detail design phase and the following term for manufacture, revaluation and testing. Instead the 1st term was used to complete a conceptual and preliminary design for the AIAA. This overran into the first month of the 2nd term. It could be perceived that too much time was consumed on completing the AIAA design phase causing the project to significantly overrun. The BMFA technical requirements were different and so conceptual and preliminary design had to be

redone. This left only 3 months to complete the entire BMFA design process. The intention was that flight test would occur in April. However, this deadline was not met, largely due to manufacturing delay. Both design iterations required nearly all components to be laser cut and the team were not permitted to do so without supervision, due to safety concerns. Therefore, a lot of time was wasted in waiting for the workshop technician. This at times delayed the project by up to 2 weeks. This time would have resulted in the flight test being completed and modifications implemented before the competition.

Project control proved to be an issue from the beginning of the project. For planning, a Gantt chart was created and applied to both terms including the manufacturing phase. However, when reaching manufacturing, delays were so great that the ground and flight tests were pushed back two months. This was beyond the teams and project managers' control and was not anticipated for. The Gantt chart was of course updated, but it brought intense pressure to the completion of tasks, with some task durations cut in half. The importance of setting defined goals and clearly outlining roles and responsibilities was emphasised on many occasions. This was in the form of individual reports to be completed every week by all team members. Meeting were held weekly for updates and review of work completed. Task deadlines were set by the project manager however, these were not always effective. Most of the team were unable to keep to these and this was partly because the time provided for tasks were too short. When deadlines were met, the work submitted was of a reduced quality. This occurred in the detail design stage of the aircraft. The pressure towards the end of the 2nd term resulted in meetings and minutes becoming less frequent and individual reports no longer deemed a priority. Retrospectively, this was a mistake. Perhaps greater recording of the detail design and manufacture process would have resulted in mistakes such as incorrect flap and aileron sizing being detected.

The team consisted of very strong personalities and so conflicts in communication was experienced continuously. Communication breakdown affected both work progress and quality. A WhatsApp group was created early on for all team members, to ensure a direct line of communication. As in any project, conflicts transpired, however by obligation these were quickly resolved as members were often required to collectively complete a task.

7.3 Resource Review

A variety of skills and preparation was required throughout the design project. Skills required included retrieving and implementing previous knowledge of engineering disciplines such as aerodynamics, propulsion, flight dynamics, manufacture and structural analysis. Many software packages were also used such as MATLAB, SolidWorks, Excel and XFLR. All team members utilized SolidWorks and Excel at one point during the project. Although the level of skill in these varied, all team members were capable of completing the tasks which incorporated these programmes. One skill that was considerably more difficult than

anticipated was time management and communication. When lack of communication occurred, this affected the ability of individuals to meet deadlines as the majority of tasks were dependant on other task values. For example, in the 1st term communication breakdown between the team responsible for the aircraft sizing chart and aerodynamic analysis resulted in the wrong speed and wing chord length being analysed. This lead to the aerodynamic analysis being repeated and the deadline not being met. After this, more care and preparation was put into forestalling similar occurrences, such as limiting the amount of file versions and daily discussions on the WhatsApp group.

Skills in manufacture were particularly improved as most of the team had not completed any manufacture related tasks since the second year. All team members have acquired far more manufacturing capabilities than when first starting the design project. One of the factors in the aircraft crashing during flight test was inaccuracy in the wing build. This was a lesson learnt through a heart-breaking experience. In the upcoming redesign along with any future engineering venture, the importance of manufacturing precision will no longer be taken by a pinch of salt by all involved.

The aero wind tunnel lab was employed for the manufacturing phase. Computer rooms, when required, were booked by supervisor Professor Atkin. This was mainly for the conceptual and preliminary phase. Room facilities were never an issue, there was always a space provided for work to be completed. Both Professor Atkin and Dr Jagadeesh provided sufficient guidance when required. In the beginning of the design project, the team required greater assurances in decision making, mainly due to lack of confidence, and the supervisors were receptive to this. However, assistance from workshop technicians during manufacturing took a considerable amount of time. The workshop health and safety regulations at City, University of London do not allow students to use the laser-cutting machine alone. Consequently, in order for any component cutting to take place, the job had to be logged with the workshop technician. There was only one workshop technician who had many other responsibilities handling the laser-cutting machine. For these reasons, it often took weeks to complete one laser-cutting task. An improvement to the process would have resulted in valuable time being gained.

7.4 Education Review

The learning outcomes in regard to proving existing aeronautical and engineering knowledge in the design of a working air vehicle was met successfully. The majority of the team were highly aware of all tasks associated with the completion of the final design. This was accomplished by allowing all team members to participate in a handful of tasks i.e. everyone designed a final component in SolidWorks. All tasks were also interrelated and thus an understanding for each process was required to complete work to a high-quality. Team work was another learning outcome met effectively. Early in the design process, it was discovered

that the combined effect of the team was greater and more efficient than individual efforts alone. With the pressure of time constraints and the desire to achieve one common goal, team work became a necessity first and a choice second. Time management was a learning outcome that was improved by all throughout the project but most certainly not perfected.

Manufacturing was experienced by all team members. In build phase, ensuring the task was completed took higher priority over the task being completed to the highest quality. This was mainly due to inexperience and time constraints. Therefore, some team members believe that the learning objective of manufacturing effectively was not accomplished. Structural testing of the final design components was also completed. The wing spar was tested to failure and a wing tip test of the final aircraft was performed. A wind tunnel test was completed on the final design and the day of the BMFA competition the flight test was completed. During the overrunning of the detail design and manufacturing process, any testing before the competition seemed unlikely. Against odds, the team were successful in completing this.

The leadership structure within the team included a project manager and project engineer. The project manager's role was to ensure deadlines were met, communication was frequent and organisation of people and resources. Many organisational resources were generated to aid in this from Gantt charts to detailed submission plans. Deadlines were enforced and monitored. The project engineer's responsibility was the management of technical and functional requirements in the design process. This was accomplished through consistent help and advice in all tasks associated with technical requirements. The BMFA design process was completed well in a short period of time and team members did not concede in effort throughout the project. For this reason, it can be deemed that leadership outcomes were met.

8 Project Summary

The aero design project 2018 involved 6 team members with the aim to design, build and fly an aircraft for the BMFA competition. This project greatly encompassed the largest variety of skills and knowledge than ever experienced in previous years at City, University of London. The project began with completing conceptual and preliminary design analysis for the AIAA. This year the aero design team were one of the first to complete an in-depth analytical scoring study, comprised of 7 DoF. The configuration determined based on this scoring algorithm was discovered to be similar to that of the winning concept. The project then shifted to the BMFA which led to the conceptual design analysis being completed for two different technical requirements. By the 2nd term, the team were confident in their ability of producing high quality conceptual tools and analysis. This left preliminary design analysis to be perfected. Aspects of aerofoil selection and empennage sizing were refined whilst new concepts were learnt such as powertrain analysis. This was a major improvement from the 1st term where

values were attained but not fully understood. The 2nd term involved harsh time constraints and so work quality was sometimes lost to meet milestones. However, the rapid work turnaround of the team allowed two full iterations to be completed, which in turn counteracted the oversights made.

As the project progressed into detailed design, it was initially steered by only two people. This was one of the poorer decisions made as it removed the aspect of team collaboration. With more members actively involved, the result could have converged towards a simpler design which was incorporated a greater level of repairability. The issue was mitigated for the second iteration where all team members participated in a detailed design task. During iterations of detailed design and manufacture, more focus should have been placed on iterating to a design with superior reparability qualities. The emphasis was always placed on the idea to build something sleek, new and unlike any aircraft developed by previous years. This resulted in some decisions of aircraft features which were unnecessary to specification requirements, such as flaps, dihedral and an aerodynamic structure which included several glue joints. The majority of team were inexperienced with manufacture, but these skills were quickly developed.

Organisation was a key aspect contributing to the successful learning outcomes of the project. Often communication breakdown would occur, and this resulted in mistakes however the nature and dynamic of the team was always to resolve issues quickly and move forward. The team would also never allow the project to be slowed down intentionally due to conflicts as there was a passion and determination to see the aircraft in operation. This goal superseded everything for all team members. There was constant support from supervisors and department advisors which encouraged and motivated the team which was particularly beneficial during times when it felt the project became stagnant. At times supervisor instructions became overloading which although frustrating at the time, retrospectively contributed to a stronger individual and team character.

On the morning of the competition the aircraft was test flown and it suffered damage beyond repair. Consequently, the team were unable to compete which was a devastating moment. Although Aquarius did not compete, the team came 3rd in the report score and 10th in the overall competition out of 16, without competing in any flights and based on the report and drawing score only. Time always felt short and one more week could have resulted in the aircraft flying at BMFA competition. The aircraft is currently still under progress as the team is dedicated to seeing the aircraft fly and land safely.

The team have all developed individually over the course of the project and have acquired an extensive amount of knowledge. This can be taken with us as we now progress into the next stage of our own journey.

References

AIAA, 2017. *AIAA DBF Previous Competitions* [Online]
Available at: https://www.aiaadbf.org/PreviousComps/
[Accessed 28 October 2017].

AIAA, 2017. *AIAA DBF. Rules.* [Online]
Available at: http://www.aiaadbf.org/
[Accessed 28 October 2017].

Atkin, C., 2015. *AE2203 Lecture 04, Flight Mechanics 1, S&L Flight.* [Online] Available at:
http://moodle.city.ac.uk/mod/resource/view.php?id=452949
[Accessed 15 October 2017].

Atkin, C., 2015. *AE2203 Lecture 09, Flight Mechanics 4, Manoeuvre, Climb Descent.* [Online]
Available at: http://moodle.city.ac.uk/mod/resource/view.php?id=452955
[Accessed 15 October 2017].

Atkin, C., 2015. AE2203 Lecture 10, Aerodynamics 4, Aerofoil Characteristics & Lift[Online]
Available at: https://moodle.city.ac.uk/mod/resource/view.php?id=452958
[Accessed Jan 15 2018].

Atkin, C., 2015. *AE2203 Lecture 11, Flight Mechanics 5, Take-Off & Landing.* [Online]
Available at: http://moodle.city.ac.uk/mod/resource/view.php?id=452956
[Accessed 16 October 2017].

Atkin, C., 2015. *AE2203 Lecture 12, Aerodynamics 5, 3D Wings* [Online]
Available at: https://moodle.city.ac.uk/mod/resource/view.php?id=452960
[Accessed Jan 15 2018].

Atkin, C., 2015. *AE2203 Lecture 13, Design 3, Sizing the Aircraft.* [Online]
Available at: http://moodle.city.ac.uk/mod/resource/view.php?id=452957
[Accessed November 2 2017].

Atkin, C., 2015. AE2203 Lecture 20, Design 6, Integration, Component Weights & CG . [Online]
Available at: https://moodle.city.ac.uk/mod/resource/view.php?id=452968
[Accessed October Dec 5 2017].

Atkin, C., 2017. ETM071 Lecture 02 Electric Propulsion . [Online]
Available at: https://moodle.city.ac.uk/mod/resource/view.php?id=851328
[Accessed October Feb 13 2018].

Brandt, Steven A. Stability and Control. *Introduction to Aeronautics: A Design Perspective.* s.l. :
AIAA, 2004.

BMFA. British Model Flying Association - Payload Challenges - Challenge 5 Weight. [Online]
2018. Available at: http://payloadchallenge.bmfa.org/the-challenges/challenge-5-weight.
[Accessed: 28 Jan 2018.]

Appendices

Rules

Circuit: The aircraft must fly two circuits every round which incorporates a 360° turn in the opposite direction during the second circuit. There is a 6mins flight time slot per round.

Take-Off: The aircraft accelerates on the ground until rotation. The motor is at its maximum allowable power output. The take-off distance is 61m.

Climb: The second flight segment requires the aircraft to climb to a safe cruise altitude.

Cruise: Cruise occurs at a constant altitude. Full throttle is not required as there are no scoring benefits to completing a lap in the quickest time.

Turn: A turn should be sustained at constant speed. A maximum load factor of 1.41 is experienced at this stage.

Landing: The aircraft must touch down in the designated landing area which is 122m in length. The rate of descent is controlled through motor power reduction.

Liquid Payload: carried in a removable container mounted internally and fully enclosed within the airframe. Payload receptacle must weight less than 10% of filled mass.

Rounds: A 6-minute time slot is allocated for each round. An attempt starts when the aircraft begins its take-off roll. A team which successfully completes qualification in the second round can attempt the 4.5kg lift in the third round.

1. **First Round:** Qualification flight. Flight without any payload or payload receptacle. 30 points awarded for successful completion.
2. **Second Round:** Complete a flight with a maximum payload of 2.25kg.
3. **Third Round:** Complete a flight with a maximum of 4.5kg.

Scoring: Awarded if aircraft completes required flight pattern and land within the designated area. 30-point penalty for substitution of major parts i.e. complete airframe, fuselage, wing or empennage.

Fuse Unit: Located a minimum of 100mm away from the propeller arc.

Configuration: Fixed wing design and specified propulsion unit. One E-Flight Power 10 motor and one E-flight 40A speed controller. Battery pack must be a 3S LiPo with a capacity not to exceed 2200mah.

Wind Speed

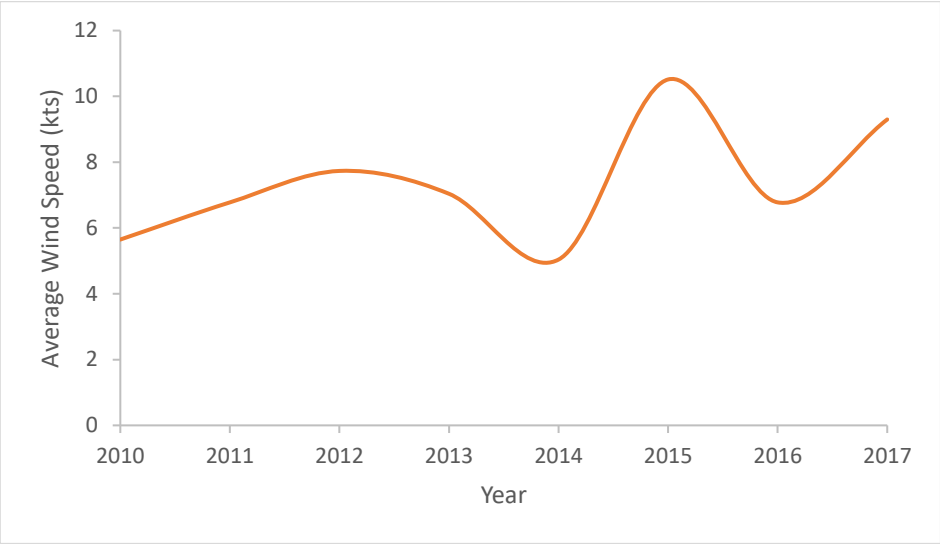

Figure A 1: Wind speed in Lincolnshire every June from 2010.

PBS	Tasks	Start	End	Duration (Days)	% Complete	Working Days	Days Complete
	BMFA COMPETITION 2018						
2	**Conceptual Design Phase**	15/01/2018	25/01/2018	11	100%	9	11
2.1	In-depth reading on BMFA rules	15/01/2018	18/01/2018	4	100%	4	4
2.2	Scoring analysis	19/01/2018	25/01/2018	7	100%	5	7
2.3	Aircraft sizing (V, W, S & P) tools	19/01/2018	27/01/2018	9	100%	6	9
2.4	Design point & first weight estimate	28/01/2018	10/02/2018	14	100%	10	14
2.5	Aerofoil analysis & selection	19/01/2018	25/01/2018	7	100%	5	7
3	**Preliminary Design Phase**	26/01/2018	27/02/2018	33	100%	23	33
3.1	Wing planform and tail plane sizing finalised	26/01/2018	08/02/2018	14	100%	10	14
3.2	Configerations & materials (sketches on SOLIDWORKS)	09/02/2018	22/02/2018	14	100%	10	14
3.3	Propulsion selection: battery, motor & prop (Inc. testing)	13/02/2018	17/02/2018	5	100%	4	5
3.4	CG calculation (fwd. and aft.)	23/02/2018	26/02/2018	4	100%	2	4
3.5	Implementation of electrics	18/02/2018	03/03/2018	14	100%	10	14
3.6	Preliminary design review V1	23/02/2018	24/02/2018	2	100%	1	2
3.6	Detail design V1	25/02/2018	27/02/2018	3	100%	2	3
4	**Procurement Plan & Ordering**	23/02/2018	03/03/2018	9	100%	6	9
4.1	Procurement plan V1	23/02/2018	27/02/2018	5	100%	3	5
4.2	Material order V1	28/02/2018	03/03/2018	4	100%	3	4
5	**Manufacturing Final**	06/03/2018	12/03/2018	7	100%	5	7
5.1	V1 build	06/03/2018	12/03/2018	7	100%	5	7
6	**Design Freeze**	13/03/2018	31/03/2018	19	100%	14	19
6.1	Critical design review V1	13/03/2018	19/03/2018	7	100%	5	7
6.2	Re-evaluation V1	20/03/2018	31/03/2018	12	100%	9	12
7	**Final Procurement Plan & Ordering**	01/04/2018	06/04/2018	6	100%	5	6
7.1	Final procurment plan V2	01/04/2018	04/04/2018	4	100%	3	4
7.2	Final material order V2	04/04/2018	06/04/2018	3	100%	3	3
8	**Manufacturing Final**	07/04/2018	19/04/2018	13	100%	9	13
8.1	V2 build	07/04/2018	19/04/2018	13	100%	9	13
9	**Testing**	23/04/2018	07/05/2018	15	33%	11	5
9.1	Structural	23/04/2018	26/04/2018	4	100%	4	4
9.2	Aerodynamic	30/04/2018	01/05/2018	2	0%	2	0
9.3	Ground & flight test	01/05/2018	07/05/2018	7	0%	5	0

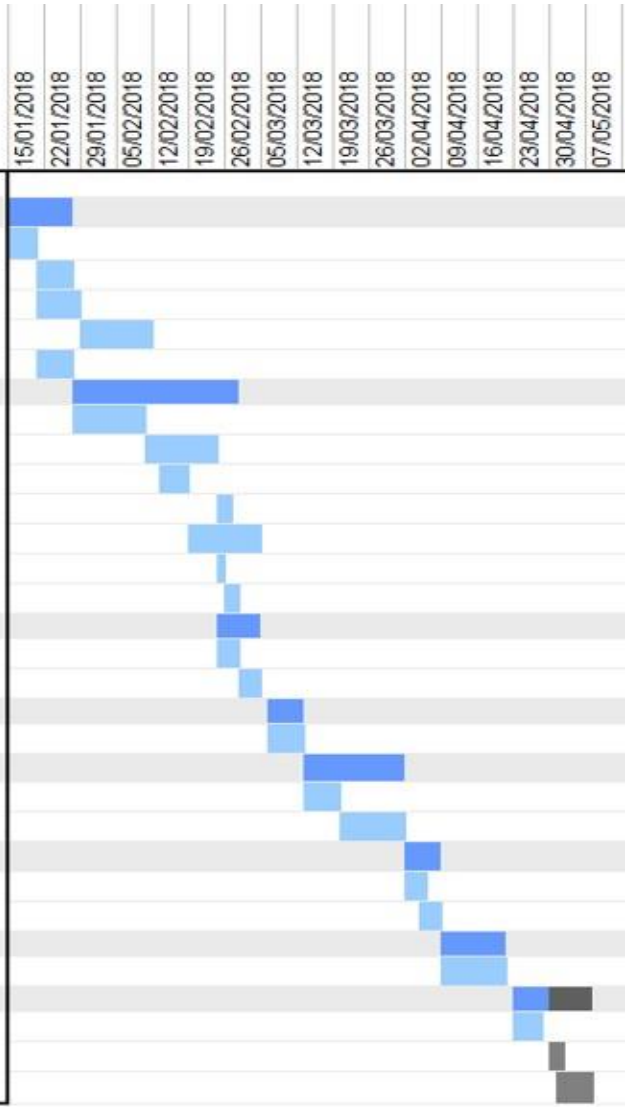

Figure A 2: Gantt Chart.

PAYLOAD (KG)	PAYLOAD (N)	MTOW (N)	OWE (N)	SCORE
0	0.000	3.147	1.489	0.000
0.2	1.962	5.805	2.185	71.840
0.4	3.924	8.463	2.881	108.961
0.6	5.886	11.121	3.577	131.633
0.8	7.848	13.779	4.273	146.918
1	9.810	16.437	4.970	157.921
1.2	11.772	19.096	5.666	166.220
1.4	13.734	21.754	6.362	172.702
1.6	15.696	24.412	7.058	177.906
1.8	17.658	27.070	7.754	182.176
2	19.620	29.728	8.450	185.742
2.2	21.582	32.387	9.147	188.765
2.4	23.544	35.045	9.843	191.360
2.6	25.506	37.703	10.539	193.613
2.8	27.468	40.361	11.235	195.586
3	29.430	43.019	11.931	197.329
3.2	31.392	45.677	12.628	198.880
3.4	33.354	48.336	13.324	200.269
3.6	35.316	50.994	14.020	201.520
3.8	37.278	53.652	14.716	202.652
4	39.240	56.310	15.412	203.683
4.2	41.202	58.698	16.277	202.441
4.4	43.164	61.626	16.974	203.441
4.6	45.126	64.285	17.670	204.309

Table A 3: Payload, weight and flight score relation.

AIRCRAFT MODEL	MTOW (KG)	MTOW (N)	OWE (INC. BATT) (KG)	WBATT (KG)	OWE (N)
BAREBACK (2002-2003)	5.35	52.48	3.08	0.590	24.427
WAZZUGER FLIEGER (2004-2005)	5.63	55.23	2.91	0.544	23.210
AIAA (1997-1998)	6.75	66.22	3.35	1.130	21.778
UNSTABLE MABLE (2004-2005)	5.28	51.80	2.56	0.340	21.778
THE TEXAS TALL BOY (1997-1998)	6.83	67.00	3.18	1.120	20.209
AEROSHOCK (2007-2008)	8.53	83.68	2.40	0.680	16.873
PEPE (1997-1998)	6.25	61.31	2.84	1.130	16.775
CORNELL UNIVERSITY (2012-2013)	3.35	32.88	1.98	0.336	16.149
RAYTHEON (2007-2008)	1.89	18.54	1.72	0.272	14.205
REDHAWKS (2012-13)	3.42	33.53	2.06	0.680	13.505
IRVINE (2012-13)	3.38	33.16	2.01	0.639	13.430
IRVINE (2014-15)	3.98	39.02	1.73	0.765	9.449
IRVINE (2013-14)	2.80	27.43	1.43	0.467	9.435
SAN DIEGO (2012-13)	3.19	31.31	1.60	0.680	9.065

Table A 4: AIAA DBF aircraft data.

Equation 6 Load factor

$$n = \frac{C_{L,BANKED}}{C_{L,S\&L}}$$

Equation 7 Cruise constraint

$$\frac{P}{W} = C_{D0} q V_{cr} \left(\frac{W}{S}\right)^{-1} + \frac{K}{q}\frac{W}{S} n^2 V_{cr}$$

Equation 8 Stall wing loading constraint

$$\frac{W}{S} = \frac{1}{2}\rho {V_{stall}}^2 C_{L\,MAX}$$

Equation 9 Take-off constraint

$$\frac{P}{W} = C V_{TO} \frac{W/S}{S_{TOFL}} \frac{1}{\sigma C_{L\,MAX}}$$

Where σ is the density ratio, estimated to be 1 for this design.

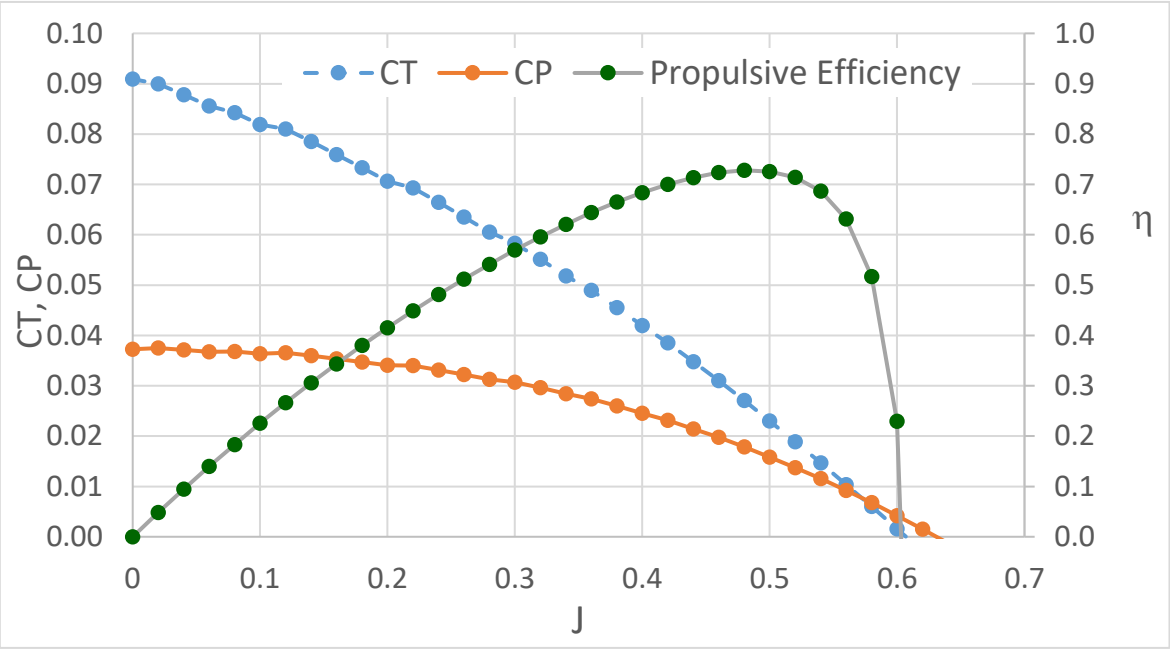

Figure A 5: C_T, C_P and η_p of 12x6" propeller

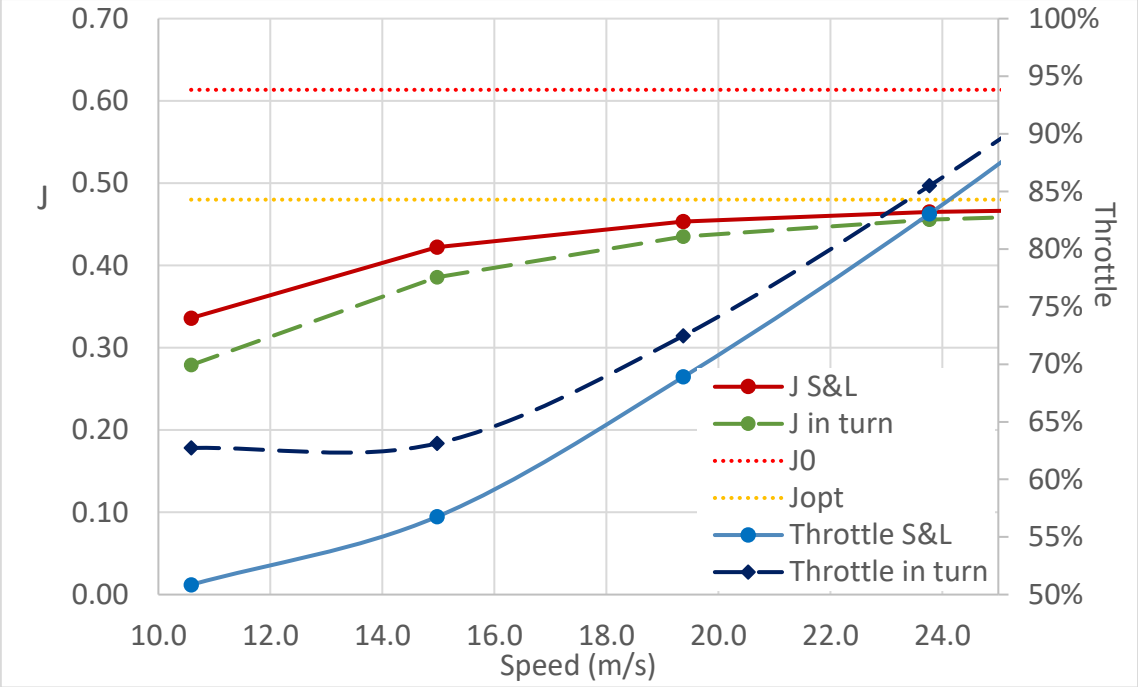

Figure A 6: J and Throttle map for 12x6" propeller

Equation 10 Servo Torque

$$Torque\ (oz-in) = \frac{(8.5 \times 10^{-6}) C^2\ V^2 S \sin(\theta_1) \tan(\theta_1)}{\sin(\theta_2)}$$

Whereby C, is the chord length (cm), V is the flight speed (mph), S is the span length (cm), Θ_1 is the control surface angle and Θ_2 is the servo angle.

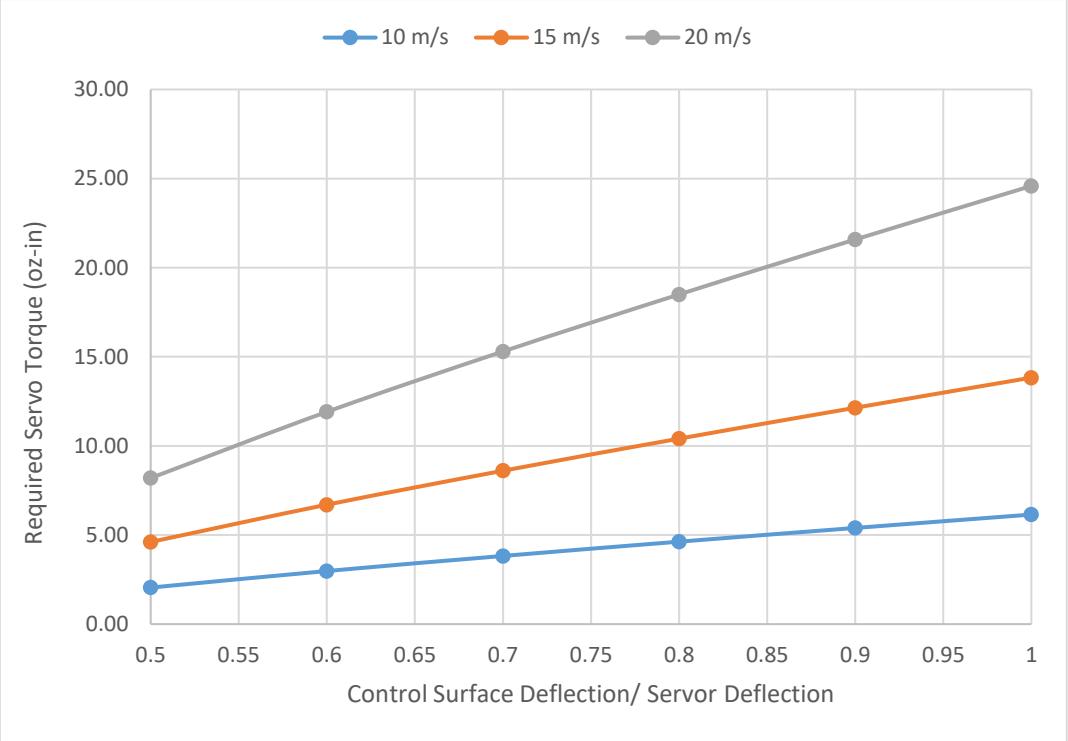

Figure A 7:Relationship between control surface/servo deflection and required torque for different flight speeds.

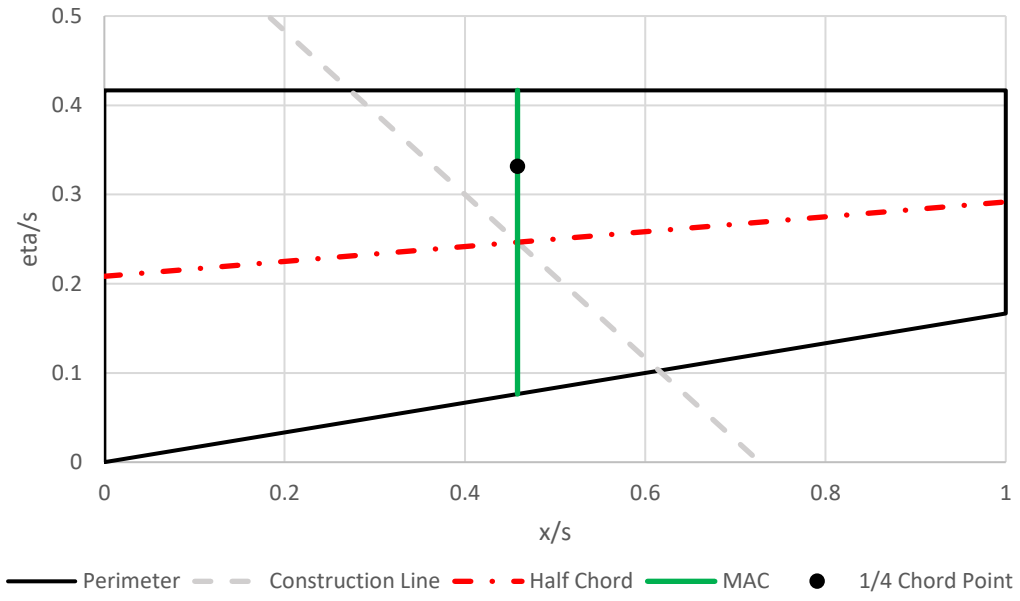

Figure A 8: Normalised wing planform.

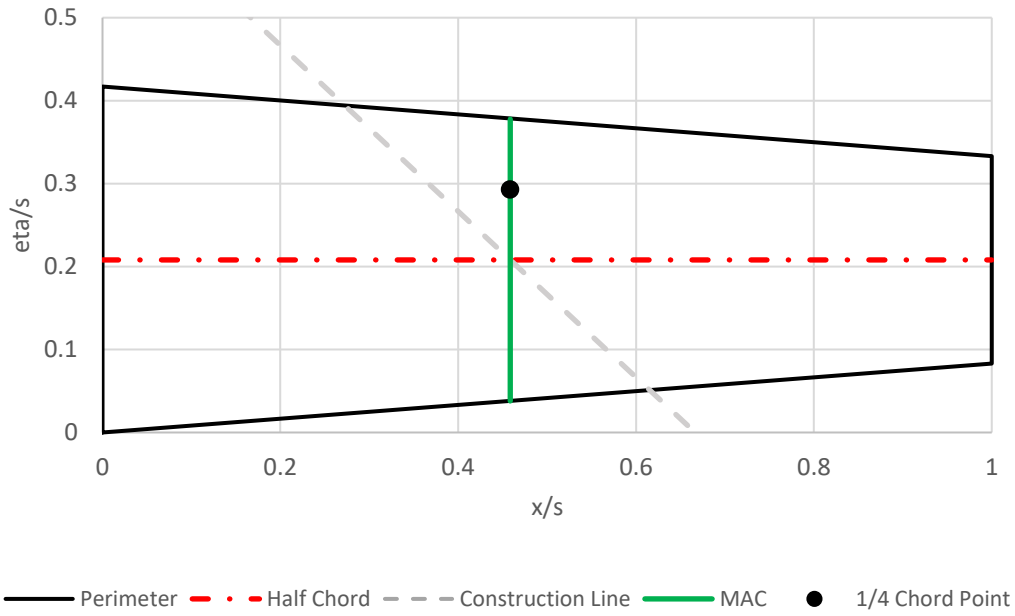

Figure A 9: Normalised wing planform adjusted to reflect actual wing planform during detail design and manufacture.

The wing planform is normalised and scaled using

$$s = \frac{b}{2}$$

Whereby s is the semi-span which is equal to 1 on the planform graph above

Equation 11 Aileron rolling moment coefficient

$$C_{l_{\delta_A}}\left(\frac{1}{rad}\right) = \frac{2C_{l_{\alpha_w}}\tau C_r}{Sb}$$

$$C_{l_{\alpha_w}}$$

$$\tau = aileron\ effectiveness$$

$$C_r = root\ chord$$

Equation 12 Bank angle

$$\Phi(°) = \frac{I_{xx}}{\rho(S_w + S_{ht} + S_{vt})C_{D_r}.y_D^3}$$

$$C_{D_r} = Wing - horizontal\ Tail - Vertical\ Tail\ Rolling\ Drag\ Coefficient$$

$$y_D^3 = drag\ moment\ arm$$

Equation 13 Aircraft rolling moment

$$L_A(Nm) = \frac{1}{2}\rho V_{app}^2 S C_l b$$

$$C_l = aircraft\ rolling\ moment\ coefficeint$$

Equation 14 Steady state roll rate

$$P_{ss}(rad/sec) = \sqrt{\frac{2\,.\,L_A}{\rho(S_w + S_{ht} + S_{vt})C_{D_r}\,.\,y_D^3}}$$

Equation 15 Aircraft rate of roll rate

$$\dot{P}\left(\frac{\text{rad}}{\text{sec}^2}\right) = \frac{{P_{ss}}^2}{2\Phi}$$

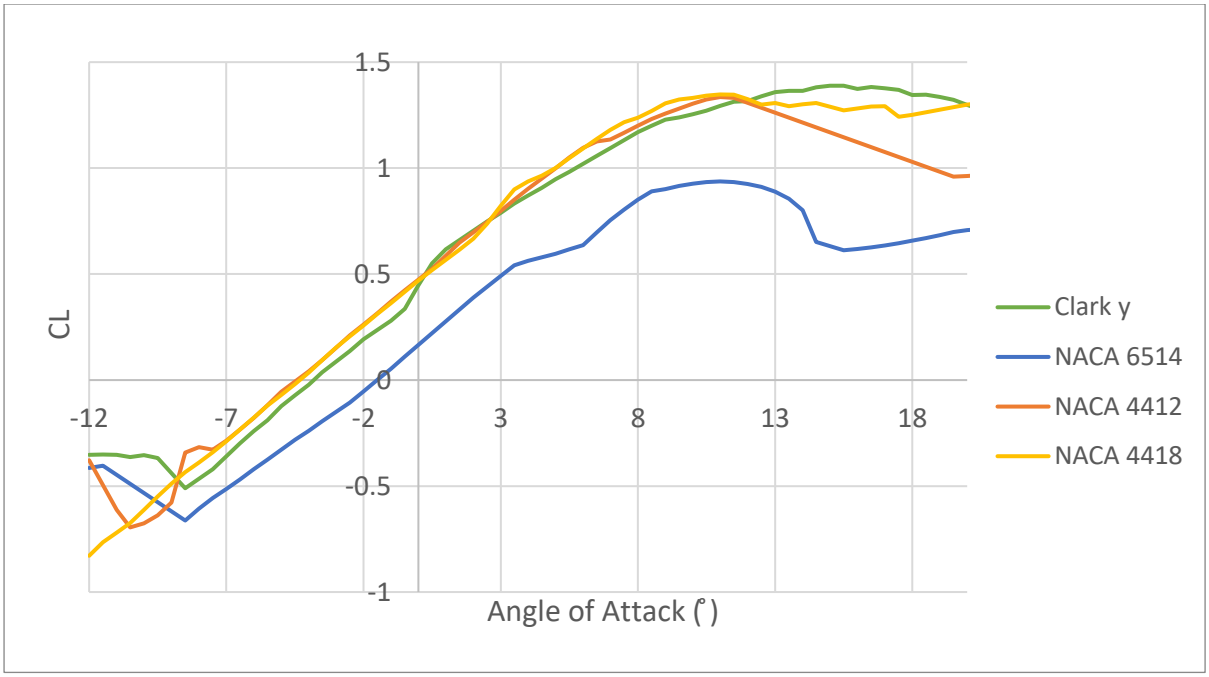

Figure A 10: Aerofoil Lift-Curve Slope Comparison at - Reynold Number: 400,000

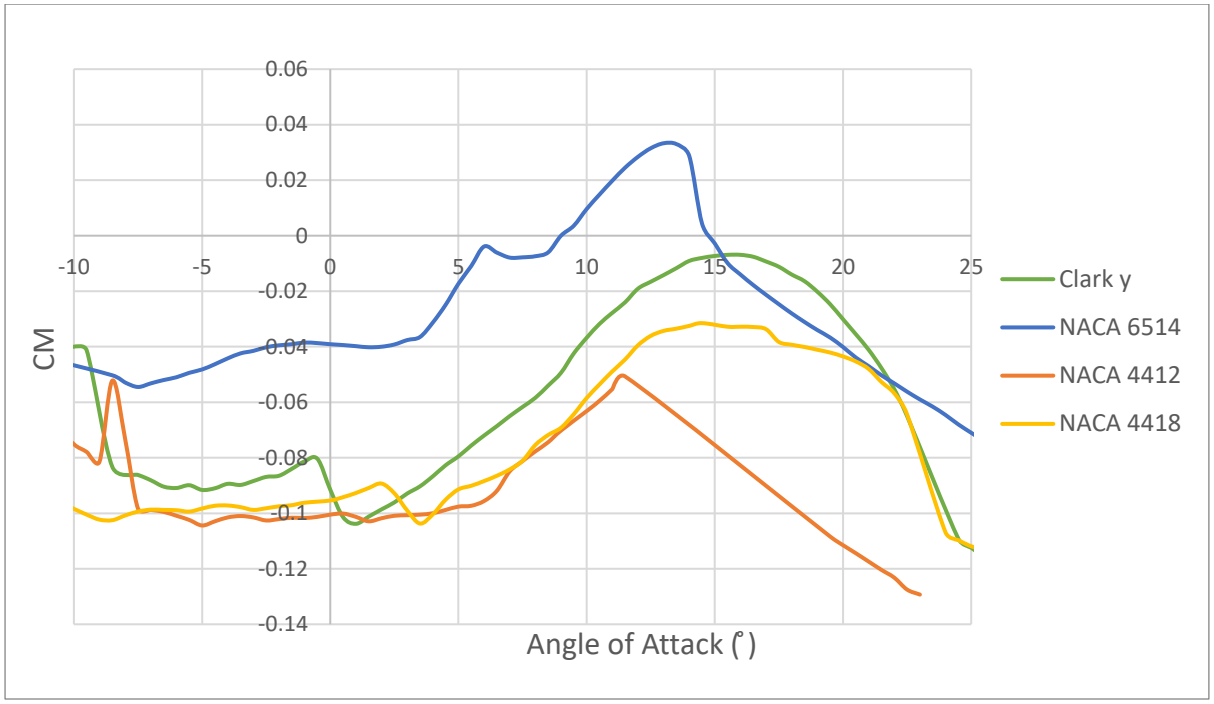

Figure A 11: Aerofoil Pitching Moment Coefficient - Reynold Number: 400,000.

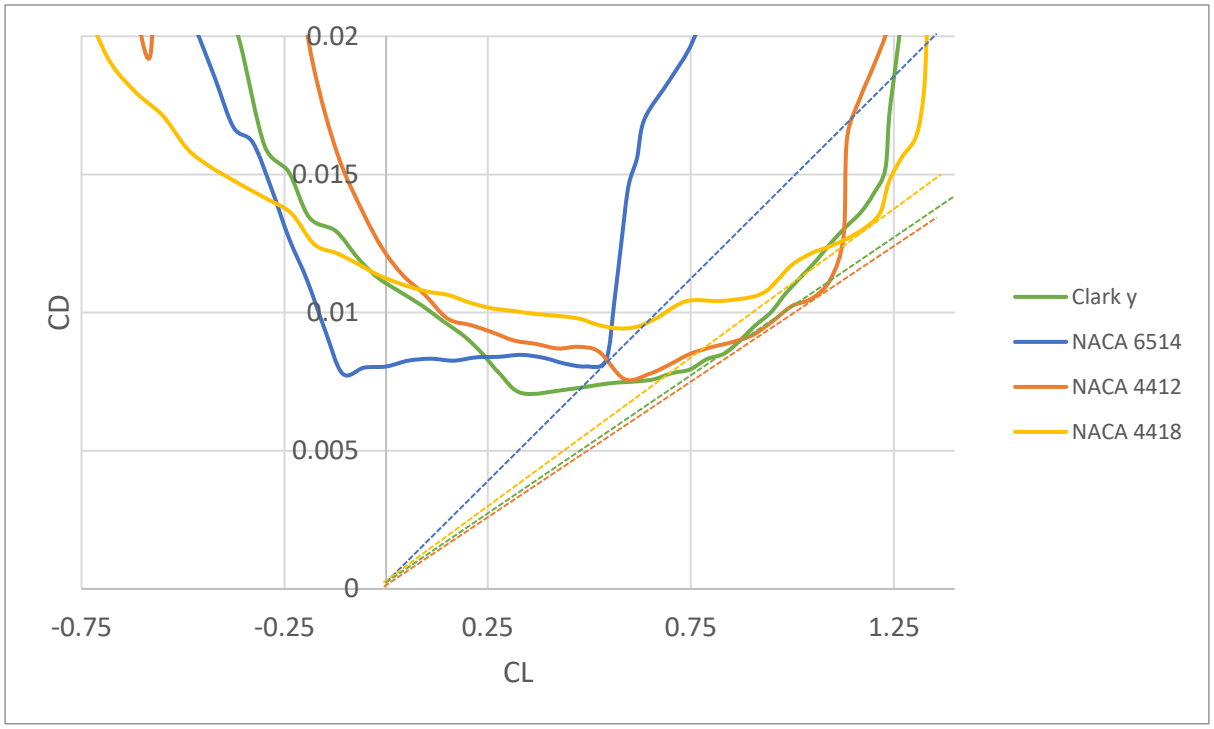

Figure A 12: Lift vs Total Drag Coefficients - Reynolds Number 400k.

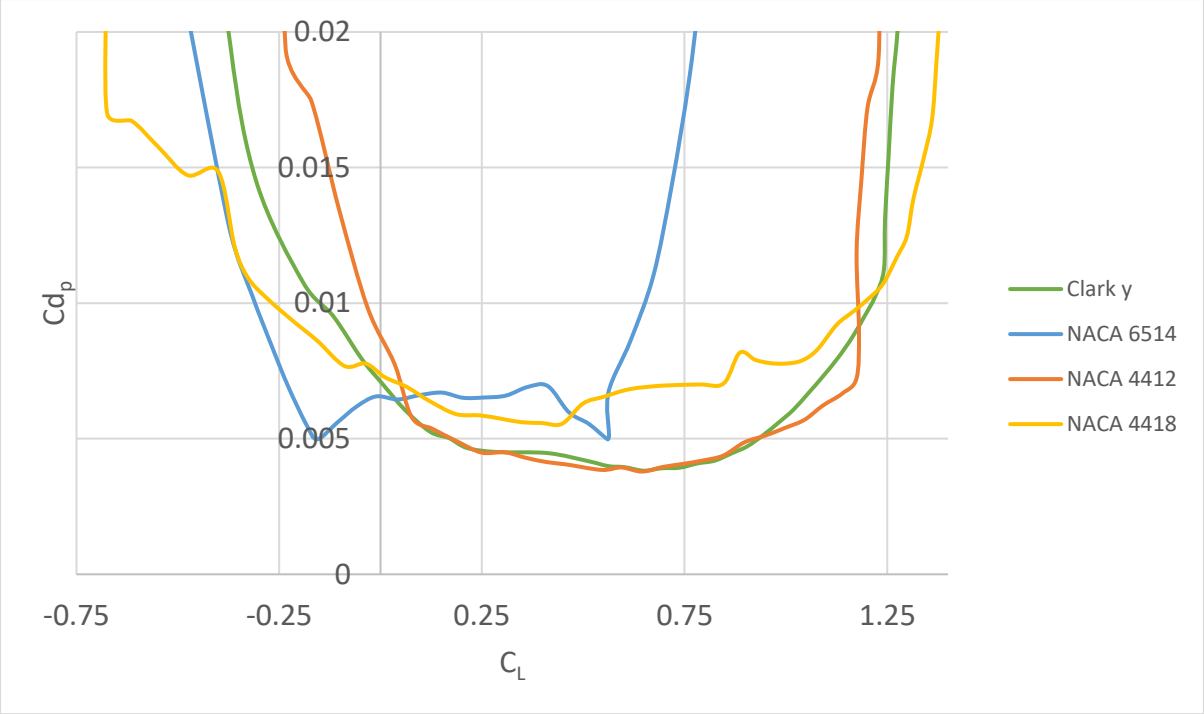

Figure A 13: Lift vs Pressure Drag - Reynolds Number 400k.

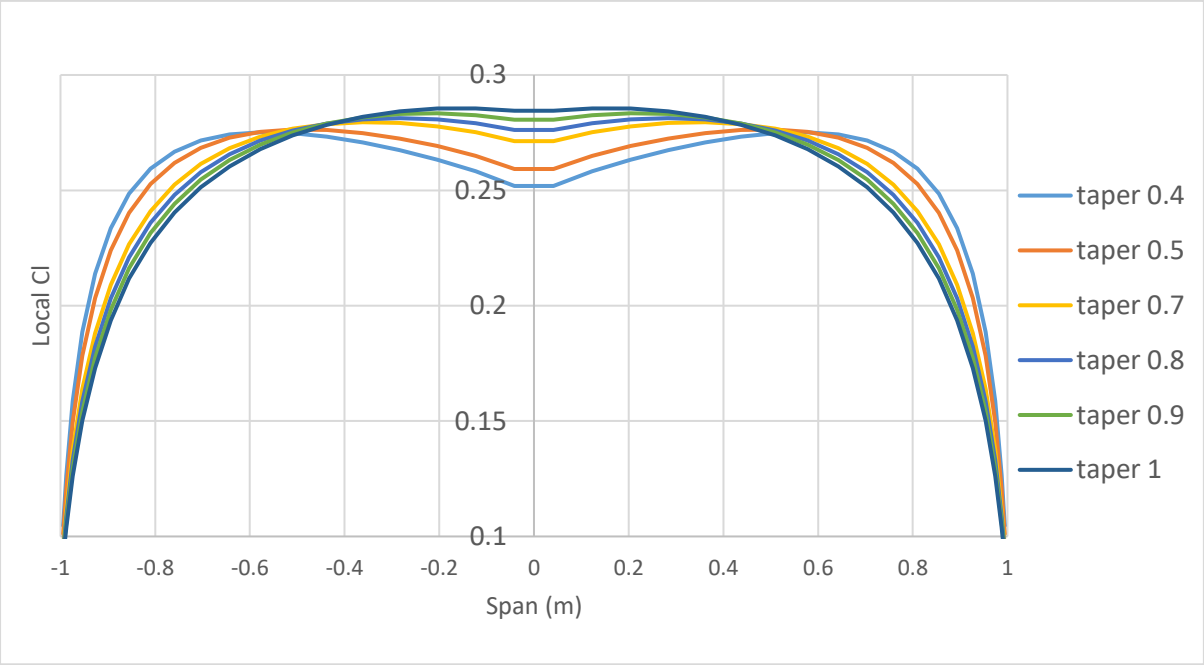

Figure A 14: Clark- Y Spanwise Lift Distribution along MAC with different Taper Ratios – Airspeed 15m/s

	AIAA			Aquarius		
Item	**Weight (kg)**	**CG (m from nose)**	**CG %MAC**	**Weight (kg)**	**CG (m from nose)**	**CG %MAC**
Boom	0.063	0.660		0.050	0.437	
Vertical Stabilizer	0.043	1.321		0.010	1.132	
Motor Mount	0.014	0.057		0.010	0.060	
Horizontal Stabilizer	0.057	1.321		0.045	1.132	
Fuselage	0.145	0.584		0.070	0.500	
Wing	0.177	0.533		0.260	0.437	
Structure Group	0.498	0.707	80.5%	0.445	0.524	97.07%
Speed controller	0.029	0.178		0.020	0.290	
Battery	0.467	0.457		0.169	0.470	
Motor	0.163	0.089		0.127	0.050	
Propeller	0.032	0.013		0.030	0.020	
Fuse/Holder	0.018	0.254		0.005	0.470	
Propulsion Group	0.710	0.336	-163.2%	0.351	0.251	-15.82%
Reciever Battery	0.090	0.254		0.060	0.470	
Reciever	0.010	0.559		0.010	0.470	
Reciever switch	0.003	0.635		0.003	0.290	
Rudder Servo	0.020	1.321		0.010	1.132	
Elevator Servos	0.020	1.321		0.010	1.132	
Ailerons Servo	0.040	0.584		0.080	0.437	
Avionics	0.181	0.582	-2.0%	0.172	0.529	98.78%
sideman Landing Gear	0.006	0.533		0.010	0.798	
Main Landng Gear	0.034	0.483		0.111	0.226	
Landing Gear	0.040	0.490	-61.9%	0.121	0.490	83.05%
Operating Weight Empty	**1.430**	**0.501**	**-55.0%**	**1.089**	**0.433**	**40.46%**

Table A 15: Preliminary CG Calculations.

Equation 16 Sample calculation for scaling wing weight W

$$W_{Aquarius} = W_{AIAA} \times \frac{Sref_{Aquarius}}{Sref_{AIAA}}$$

Equation 17 Sample calculation for scaling nose landing gear CG from nose N

$$N_{Aquarius} = N_{AIAA} + 0.14 \times N_{AIAA}$$

Equation 18 Sample calculation for scaling Structure Group CG % MAC:

$$CG_{\%MAC} = \frac{CG_{from\ nose} - 25\%MAC_{from\ nose}}{MAC + 0.25}$$

Order	Date	Quantity	Item	Cost	Sub-Total	Shipping	Total
Balsa Mart	23/02/2018	1	3/8" x 3/8" x 36" L.E. 9.5mm x 9.5mm x 915mm	£1.94			
		1	1/2" x 1/2" x 36" L.E. 12.5mm x 12.5mm x 915mm	£2.49			
		1	1/2" x 1/8" x 36" T.E. 12.5mm x 3.2mm x 915mm	£1.40			
		3	1" x 2" x 36" Balsa Block 25mm x 50mm x 915mm	£22.65			
		10	3/32" x 4" x 36" Balsa 2.4mm x 102mm x 915mm	£22.00			
		4	1/16" x 3" x 36" Balsa 1.6mm x 76mm x 915mm	£6.20			
		2	2.0mm (3/32") Marine Ply 300mm x 900mm, 1ft x 3ft	£20.94			
		1	3.2mm (1/8") Marine Ply 300mm x 900mm, 1ft x 3ft	£8.85			
		1	0.8mm (1/32") Marine Ply 300mm x 900mm, 1ft x 3ft	£12.75			
					£99.22	£7.95	£107.17
BMFA	23/02/2018	1	Entry Fee	£50.00			
					£50.00	£0.00	£50.00
Easy Composites	23/02/2018	2	Carbon Fibre Square Box 10mm (8mm) - 1m Length	£20.90			
		1	Pultruded Carbon Fibre Tube 8mm (6mm) - 1m Length	£8.60			
		1	Pultruded Carbon Fibre Tube 6mm (4mm) - 1m Length	£6.85			
		8	Pultruded Carbon Fibre Tube 2mm (1mm) - 1m Length	£14.40			
		1	VAT	£11.33			
					£62.08	£5.90	£67.98
Amazon	23/02/2018	1	4 x UHU HART ADHESIVE - MODELLING GLUE	£14.99			
					£14.99	£0.00	£14.99
Hobby King	23/02/2018	2	CA HINGE L25*W20*H0.3 (10PCS)	£1.08			
		1	CONTROL HORNS 16X20MM (10PCS)	£0.68			
		1	CONTROL HORNS 13.5X16MM (10PCS)	£0.94			
		1	ADJUSTABLE CONTROL HORN 3X34MM (5SETS)	£1.67			
		1	TURNIGY GRAPHITE POWDER DRY LUBRICANT (6G)	£2.27			
					£6.64	£4.70	£11.34
Hobby King	02/03/2018	1	CARBON FIBER LANDING GEAR	£16.34			

					£16.34	£18.01	£34.35
Balsa Mart	06/03/2018	12	3/32" x 4" x 36" Balsa 2.4mm x 102mm x 915mm	£26.40			
					£26.40	£7.95	£34.35
Kitronik	06/03/2018	3	1.5mm BR Grade Birch Laser Plywood, 600mm x 400mm	£24.12			
		5	2mm BR Grade Birch Laser Plywood, 600mm x 400mm	£54.90			
					£79.02	£7.80	£86.82
Overlander	10/03/2018	3	2200mAh 3S 11.1v 35C LiPo Battery	£42.48			
		1	VAT	£9.33			
					£51.81	£4.17	£55.98
Elite Models	10/03/2018	2	Oracover Air Outdoor 2m Transparent Red	£39.88			
		2	Oracover Air Outdoor 2m Transparent Blue	£39.88			
					£79.76	£5.99	£85.75
Hobby King	10/03/2018	4	DS65HB DIGITAL HIGH SPEED 25T 1.5KG / 0.07SEC	£17.48			
		6	TURNIGY™ BMS-380MAX 4.1KG / 0.16SEC	£69.00			
		4	TURNIGY™ TSS-9 DIGITAL 15T 1.9KG / 0.11SEC	£12.16			
			XT60 CHARGED/DISCHARGED BATT. INDICATOR CAPS	£2.16			
			TURNIGY NANO-TECH 550MAH 2S 65C LIPO PACK	£11.88			
					£112.68	£0.00	£112.68
Hobby King	17/03/2018	5	MALE T-CONNECTOR <-> FEMALE XT-60 (1PC/BAG)	£5.05			
		1	200 Reward Points	-£1.43			
					£3.62	£4.68	£8.30
Amazon	20/03/2018	3	4 x UHU HART ADHESIVE - MODELLING GLUE	£44.97			
					£44.97	£0.00	£44.97
Easy Composites	20/03/2018	10	Pultruded Carbon Fibre Tube 2mm (1mm) - 1m Length	£18.00			
		2	Pultruded Carbon Fibre Tube 6mm (4mm) - 1m Length	£13.70			
		2	Pultruded Carbon Fibre Tube 5mm (3mm) - 1m Length	£11.90			
		2	Carbon Fibre Square Box 10mm (8mm) - 1m Length	£20.90			

		24	0.28mm Micro Carbon Fibre Rod 1m Length	£38.88			
		1	VAT	£21.86			
					£125.24	£5.90	£131.14
Kitronik	26/03/2018	8	1.5mm BR Grade Birch Laser Plywood, 600mm x 400mm	£64.32			
					£64.32	£14.20	£78.52
Balsa Mart	03/04/2018	10	3/32" x 4" x 36" Balsa 2.4mm x 102mm x 915mm	£22.00			
					£22.00	£7.95	£29.95
R&R Hobbies	03/04/2018	2	BALSA WOOD 2.5mm x 155mm (6) x 17 inches x 5	£14.70			
		1	Partial Refund	-£2.50			
					£12.20	£6.65	£18.85
Glue Guns Direct	04/04/2018	1	TECBOND 263 / 12mm PP Glue Sticks	£98.45			
		1	TEC 810 12mm Glue Gun	£69.15			
		1	£10 Off over £100 discount	-£10.00			
		1	VAT	£31.52			
					£189.12	£0.00	£189.12
Direct Plastics	05/04/2018	1	Polypropylene Natural Rod 25mm dia x 500mm	£2.82			
		4	Polypropylene Natural Sheet 1000 x 500 x 1mm	£24.28			
		1	VAT	£6.61			
					£33.71	£5.95	£39.66
Balsa Mart	09/04/2018	10	1/32" x 4" x 36" Balsa 0.8mm x 102mm x 915mm	£17.00			
		5	Mini Snap Links, pack of 4 (SL878)	£14.95			
		2	14 x 7 APC Thin Electric Prop (ELP1407E)	£15.00			
		2	12 x 6 APC Thin Electric Prop (ELP1206E)	£11.30			
					£58.25	£7.95	£66.20
Kitronik	19/04/2018	6	Frosted Polypropylene Sheet 0.5mm x 1100mm x 650mm	£16.56			
					£16.56	£7.80	£24.36

Elite Models	20/04/2018	1	10 x 5.0mm x 100mm x 1m Sheet Balsa	£23.20			
		1	4 x 6mm - 1/4 INCH HARDWOOD DOWEL 5521007	£3.96			
		1	2 x Oracover Air Adhesive (0961) 100ml	£12.58			
					£39.74	£5.99	£45.73
SMC	20/04/2018	1	Solartex Fluorescent Red 2m	£16.50			
		1	Solartex Dark Blue 2m	£16.50			
					£33.00	£6.99	£39.99
Kitronik	20/04/2018	4	0.8mm BR Grade Birch Laser Plywood, 600mm x 400mm	£34.80			
		4	2mm BR Grade Birch Laser Plywood, 600mm x 400mm	£43.92			
					£78.72	£7.80	£86.52
Balsa Mart	12/06/2018	8	3/32" x 4" x 36" Balsa 2.4mm x 102mm x 915mm	£17.60			
		4	1/32" x 4" x 36" Balsa 0.8mm x 102mm x 915mm	£6.80			
					£24.40	£7.95	£32.35
			TOTAL		£1,344.79	£152.28	**£1,497.07**

Table A 16: Procurement list.